PRISM Theory of the Structure, Thermodynamics, and Phase Transitions of Polymer Liquids and Alloys

K.S. Schweizer[1] and J.G. Curro[2]
[1] Departments of Materials Science & Engineering and Chemistry, University of Illinois, Urbana, Illinois 61801, USA
[2] Sandia National Laboratories, Albuquerque, New Mexico 87185, USA

The recent development of a microscopic theory of the equilibrium properties of polymer solutions, melts and alloys based on off-lattice Polymer Reference Interaction Site Model (PRISM) integral equation methods is reviewed. Analytical and numerical predictions for the intermolecular structure and collective density scattering patterns of both coarse-grained and atomistic models of polymer melts are presented and found to be in good agreement with large scale computer simulations and diffraction measurements. The general issues and difficulties involved in the use of the structural information to compute thermodynamic properties are reviewed. Detailed application of a hybrid PRISM approach to calculate the equation-of-state of hydrocarbon fluids is presented and found to reproduce accurately experimental PVT data on polyethylene. The development of a first principles off-lattice theory of polymer crystallization based on a novel generalization of modern thermodynamic density functional methods is discussed. Numerical calculations for polyethylene and polytetrafluoroethylene are in good agreement with the experimental melting temperatures and liquid freezing densities. Generalization of the PRISM approach to treat phase separating polymer blends is also discussed in depth. The general role of compressibility effects in determining small angle scattering patterns, the effective chi-parameter, and spinodal instability curves are presented. New theoretical concepts and closure approximations have been developed in order to describe correctly long wavelength concentration fluctuations in macromolecular alloys. Detailed numerical and analytical applications of the PRISM theory to model athermal and symmetric blends are presented, and the role of nonmean field fluctuation processes are established. Good agreement between the theory and computer simulations of simple symmetric polymer blends has been demonstrated. Strong, nonadditive compressibility effects are found for structurally and/or interaction asymmetric blends which have significant implications for controlling miscibility in polymer alloys. Recent generalizations of PRISM theory to treat block copolymer melts, and nonideal conformational perturbations, are briefly described. The paper concludes with a brief summary of ongoing work and fertile directions for future research.

Advances in Polymer Science, Vol. 116

1 Introduction

Understanding the intermolecular packing, conformation, thermodynamics, and phase transitions of high polymer fluids and alloys is both a challenging problem in statistical mechanics and a subject of immense technological importance. Historically, theoretical progress has been possible only by introducing extreme approximations of both a chemical structural and statistical mechanical nature. Simple lattice models solved at the lowest mean field level represent the classical approach [1]. Recently, Freed, Dudowicz and collaborators have pioneered the development of statistical thermodynamic theories of sophisticated lattice models which can deal approximately with monomer shape effects [2]. Fluctuation corrections to the simple random mixing approximation are perturbatively computed, and many interesting results have emerged. However, the lattice restriction is still, potentially, a major limitation, especially if local, chemically specific packing effects are important. Structural properties are also not explicitly addressed. Phenomenological field theoretical and/or Landau expansion approaches have been extensively developed [3] and provide considerable qualitative insight into the general aspects of phase behavior and polymer conformation. However, such approaches heavily coarse-grain over chemical structure and often introduce a locally unrealistic incompressibility approximation. Thus, packing correlations on spatial scales of the order of and less than the statistical segment length are ignored. From a practical point of view, the presence of empirical parameters of uncertain relation to the microscopic intermolecular forces and chemical structure of specific materials limit the detailed predictive power of such theories.

A distinctly different approach, which has witnessed much progress recently, is large scale Monte Carlo and molecular dynamics computer simulations [4]. These studies provide many insights regarding the physics of model polymer fluids, and also valuable benchmarks against which approximate theory can be tested. However, an atomistic, off-lattice treatment of high polymer fluids and alloys remains immensely expensive, if not impossible, from a computational point of view.

Over the past several years we and our collaborators have pursued a continuous space liquid state approach to developing a computationally convenient microscopic theory of the equilibrium properties of polymeric systems. Integral equations methods [5–7], now widely employed to understand structure, thermodynamics and phase transitions in atomic, colloidal, and small molecule fluids, have been generalized to treat macromolecular materials. The purpose of this paper is to provide the first comprehensive review of this work referred to collectively as "Polymer Reference Interaction Site Model" (PRISM) theory. A few new results on polymer alloys are also presented. Besides providing a unified description of the equilibrium properties of the polymer liquid phase, the integral equation approach can be combined with density functional and/or other methods to treat a variety of inhomogeneous fluid and solid problems.

The outline of the paper is as follows. In Sect. 2 we describe the basic RISM and PRISM formalisms, and the fundamental approximations invoked that render the polymer problem tractable. The predictions of PRISM theory for the structure of polymer melts are described in Sect. 3 for a variety of single chain models, including a comparison of atomistic calculations for polyethylene melt with diffraction experiments. The general problem of calculating thermodynamic properties, and particularly the equation-of-state, within the PRISM formalism is described in Sect. 4. A detailed application to polyethylene fluids is summarized and compared with experiment. The development of a density functional theory to treat polymer crystallization is briefly discussed in Sect. 5, and numerical predictions for polyethylene and polytetrafluoroethylene are summarized.

The second general part of this paper describes the PRISM theory of phase-separating polymer mixtures. This aspect is less well developed than the one-component melt problem, especially with regards to its atomistic implementation for real materials. However, construction of a microscopic theory of polymer alloys is presently of great interest both scientifically and due to the technological desire to "molecularly engineer" miscibility and phase structure. The general theoretical issues for polymer blends within the PRISM framework are discussed in Sect. 6. Specific applications to model athermal polymer mixtures are summarized in Sect. 7. Section 8 treats thermally-induced phase separating blends, and the subtle question of the appropriate closure approximation is discussed. New "molecular-based" closure approximations are described, and representative results for model symmetric polymer blends are presented and compared with recent Monte Carlo simulations. Analytical results are also presented for stiffness and interaction potential asymmetric blends where non-additive compressibility effects are found to be very important. PRISM theory of periodic block copolymers is briefly described in Sect. 9. Section 10 discusses the generalization of PRISM methodology to allow an ab initio assessment of "nonideal" conformational effects. The paper concludes with a brief overview of ongoing and future directions.

2 PRISM Theory

The theoretical approach we take to describe amorphous polymer liquids is based on integral equation theory which has its roots in the theory of monatomic liquids [5]. Consider for a moment a uniform system of n spherical particles of density $\rho = n/V$. A convenient measure of the degree of order in such a system is the radial distribution function g(r) defined as

$$\rho^2 g(r) = \left\langle \sum_{i \neq j=1}^{n} \delta(\vec{r}_i)\delta(\vec{r} - \vec{r}_j) \right\rangle . \tag{2.1}$$

Physically $\rho g(r)$ is the density of particles at distance r from a given particle. Most thermodynamic properties of interest can be computed from a knowledge of g(r) and the interparticle pair potential v(r). The starting point in calculating the radial distribution function is the well known Ornstein-Zernike equation [5]:

$$h(r) = C(r) + \rho\int C(|\vec{r} - \vec{r}'|)h(r')d\vec{r}' \tag{2.2}$$

where $h(r) = g(r) - 1$ is frequently called the total correlation function and approaches zero at large r. Equation (2.2) serves as a definition for the direct correlation function C(r) which plays a central role in liquid state physics.

Unfortunately C(r) does not have a readily apparent physical interpretation. However, some insight [5, 6] can be gained by iterating Eq. (2.2) in explicit order of density

$$h(r) = C(r) + \rho C*C(r) + \rho^2 C*C*C(r) + \rho^3 C*C*C*C(r) + \cdots \tag{2.3}$$

where the * operator denotes the convolution integral following standard notation. We may interpret this equation as follows: two given particles at distance r apart are correlated "directly" from the first term on the RHS of Eq. (2.3); subsequent higher order terms in density represent "indirect" correlations between the two given particles mediated by the remaining particles in the system. At low density, high temperature, or large separation the direct correlation function is exactly related to the pair potential as $C(r) = \exp[-\beta v(r)] - 1 \cong -\beta v(r)$ where $\beta = 1/k_B T$ and k_B is Boltzmann's constant. At higher densities C(r) is strongly modified due to many-particle effects. However, it can be argued [5, 6] that C(r) still has roughly the same range as v(r) itself and is a simpler object to approximate than h(r). Since Eq. (2.3) shows that h(r) can be expressed as an expansion in C(r), one can view the direct correlation function, for qualitative purposes, as an effective or renomalized pair potential which accounts for the many body contribution to h(r).

The expectation that C(r) is a short range, relatively "simple" function can be exploited to develop a second approximate relationship, or closure relation, between h(r) and C(r). Based on graph theoretical techniques [5] or functional expansions [5, 7], one can deduce the Percus-Yevick approximation:

$$C(r) \cong \{1 - \exp[\beta v(r)]\}g(r) \equiv \{\exp[-\beta v(r)] - 1\}y(r) \tag{2.4a}$$

where the "indirect" correlation function, y(r), is a continuous and finite function for all values of r. For hard spheres of diameter d, Eq. (2.4a) takes the simple form

$$\begin{aligned} g(r) &= 0 \quad r < d \\ C(r) &\cong 0 \quad r > d \ . \end{aligned} \tag{2.4b}$$

The first condition on g(r) inside the hard core is an exact statement of the impenetrability of hard spheres. The second condition on C(r) outside the hard core is approximate and emphasizes that C(r) and v(r) have roughly the same

spatial range. Equations (2.4) plus the Ornstein-Zernike equation, Eq. (2.2), lead to the well-known Percus-Yevick integral equation theory that has been successful [5] in describing the structure of monatomic liquids with strongly repulsive and weakly attractive interactions.

These integral equation ideas of monatomic liquids were generalized and applied to molecular liquids by Chandler and Andersen [6, 8] to formulate the Reference Interaction Site Model or RISM theory of molecular fluids. In the RISM approach, each molecule is subdivided into spherically symmetric, interaction sites. The intermolecular pair structure of a uniform molecular liquid of M molecules is now specified through a site-site radial distribution function matrix $g_{\alpha\gamma}(r)$:

$$\rho^2 g_{\alpha\gamma}(r) = \left\langle \sum_{i \neq j=1}^{M} \delta(\vec{r}_i^{\,\alpha})\delta(\vec{r} - \vec{r}_j^{\,\gamma}) \right\rangle . \tag{2.5}$$

In Eq. (2.5), ρ is the number density of molecules and $\vec{r}_i^{\,\alpha}$ is the position vector of site α on molecule i. It can be seen from Eq. (2.5) that $g_{\alpha\gamma}(r)$ is the intermolecular radial distribution function for sites α and γ on different molecules. Chandler and Andersen generalized the Ornstein-Zernike equation to reflect the fact that in molecular liquids, unlike monatomic liquids, there exist intramolecular correlations. This generalized Ornstein-Zernike-like, or RISM, equation has the form [6, 8]

$$\underline{\underline{h}}(r) = \iint d\vec{r}_1 d\vec{r}_2 \underline{\underline{\omega}}(|\vec{r} - \vec{r}_1|)\underline{\underline{C}}(|\vec{r}_1 - \vec{r}_2|)[\underline{\underline{\omega}}(r_2) + \rho\underline{\underline{h}}(r_2)] \tag{2.6}$$

where $\underline{\underline{h}}(r)$, $\underline{\underline{C}}(r)$, and $\underline{\underline{\omega}}(r)$ are $N \times N$ matrices (for molecules consisting of N sites) with matrix elements $h_{\alpha\gamma}(r) = g_{\alpha\gamma}(r) - 1$, $C_{\alpha\gamma}(r)$, and $\omega_{\alpha\gamma}(r)$, respectively. The functions $h_{\alpha\gamma}(r)$ and $C_{\alpha\gamma}(r)$ are intermolecular correlations functions between sites on different molecules. In contrast, $\omega_{\alpha\gamma}(r)$ is the intramolecular probability density between a pair of sites on the same molecule. For molecules composed of hard sphere sites the closure for RISM theory is carried over by analogy with the Percus-Yevick closure of monatomic liquids.

$$\begin{aligned} g_{\alpha\gamma}(r) &= 0 \quad r < d_{\alpha\gamma} \\ C_{\alpha\gamma}(r) &\cong 0 \quad r > d_{\alpha\gamma} \ . \end{aligned} \tag{2.7}$$

Equations (2.6) and (2.7) form a set of nonlinear integral equations which can be solved by standard numerical techniques [5, 9]. Thus, by solution of these integral equations, one can obtain a quantitative description of the short range, intermolecular packing in the liquid state which includes the effect of the intramolecular bonding constraints. Chandler and coworkers used this RISM formalism to study various small, rigid polyatomic liquids [9, 10] and found good agreement with computer simulation and scattering experiments for the intermolecular structure.

We have generalized the RISM formalism to describe the structure of flexible polymer chain liquids [11–15]. The application of RISM theory to polymers is

referred to as polymer RISM, or PRISM, theory. (Note that there is no connection with the well known *rotational isomeric state model* commonly employed to calculate the intramolecular structure of isolated polymer chains [16].) In the case of rigid molecules, the intramolecular probability functions $\omega_{\alpha\gamma}(r)$ are simply delta functions which specify the positions of the atoms or sites on the molecule. When the PRISM theory is applied to flexible polymers, a difficulty arises because in general the intramolecular functions $\omega_{\alpha\gamma}(r)$ and the intermolecular radial distribution functions $g_{\alpha\gamma}(r)$ depend on each other [6]. A rigorous calculation would thus require that the intramolecular and intermolecular structure be determined self consistently. This general problem is discussed in Sect. 10. For one-component polymer melts, we can avoid this difficult self-consistent calculation, at least nominally, by invoking the Flory *ideality hypothesis* [17]. The *intra*molecular excluded volume forces that tend to expand a polymer chain in dilute solution are nominally cancelled in the melt by *inter*molecular excluded volume interactions. The net result of these two opposing effects is that the polymer melt acts as a theta solvent for itself and the average intramolecular structure of a chain is ideal. There is ample evidence that these ideas are substantially correct based on computer simulations [18] and neutron scattering experiments [19] on polymer melts. Within this approximation the intramolecular structure can be calculated from an "ideal" single chain model without long range excluded volume interactions [16]. The result of this single chain calculation is then used as input to the PRISM theory to compute the intermolecular correlation functions $g_{\alpha\gamma}(r)$ and $C_{\alpha\gamma}(r)$ in the polymer melt.

Inspection of the generalized Ornstein-Zernike-like equations reveals that, for an ideal chain molecule fluid consisting of N(even) identical (but still symmetry nonequivalent) sites, the matrix equation, Eq. (2.6), consists of $N(N+2)/8$ independent integral equations. The large number of coupled integral equations results from the fact that the correlation functions $g_{\alpha\gamma}(r)$ depend on the specific locations of site α on one chain and site γ on another chain. For a polymer the number of equations would obviously become unmanageably large. We can argue [13], however, that, for long polymer chains, end effects can be neglected, and thus all the sites on a homopolymer chain can be treated as equivalent. This simplification is exact for a ring homopolymer [12]. Such an equivalent-site approximation leads to a considerable mathematical simplification and renders the calculation of the structure of polymer melts a tractable problem. A computationally tractable scheme for computing "chain end" corrections has also been formulated [13]. Taking all the sites as equivalent on average allows us to write

$$h(r) = g(r) - 1 = h_{\alpha\gamma}(r)\,,$$

$$C(r) = C_{\alpha\gamma}(r)\,. \tag{2.8a}$$

With this simplification, and subsequent preaveraging over the intramolecular structure, the generalized Ornstein-Zernike-like matrix equations reduce to

a single scalar equation of the form

$$h(r) = \int\int d\vec{r}_1 d\vec{r}_2 \omega(|\vec{r} - \vec{r}_1|) C(|\vec{r}_1 - \vec{r}_2|)[\omega(r_2) + \rho_m h(r_2)] \tag{2.8b}$$

where ρ_m is the site density $N\rho$, and $\omega(r)$ is defined as the intramolecular distribution averaged over all pairs of sites on a single chain, and

$$\omega(r) = \frac{1}{N} \sum_{\alpha,\gamma=1}^{N} \omega_{\alpha\gamma}(r) . \tag{2.9}$$

Since it is the second relation in Eq. (2.8a) which is the fundamental approximation, $h(r)$ in Eq. (2.8b) can be rigorously interpreted as the "average" correlation function, i.e. $h(r) = N^{-2} \sum_{\alpha\gamma}^{N} h_{\alpha\gamma}(r)$. Recent work has demonstrated that the equivalent site approximation is remarkably accurate for $h(r)$, even for very short alkanes such as propane [20] ($N = 3$) and butane [21] ($N = 4$).

For hard core homopolymers, $d = d_{\alpha\gamma}$ and the Percus-Yevick/RISM closure of Eq. (2.7) applies. Using the convolution theorem for Fourier transforms, Eq. (2.8b) can be conveniently written as

$$\hat{h}(k) = \hat{\omega}^2(k)\hat{C}(k) + \rho_m \hat{\omega}(k)\hat{C}(k)\hat{h}(k) \tag{2.10}$$

where the caret denotes Fourier transformation with wave vector k. $\hat{\omega}(k)$ is the Fourier transform of Eq. (2.9) and can be identified with the single chain structure factor:

$$\hat{\omega}(k) = \frac{1}{N} \sum_{\alpha,\gamma=1}^{N} \hat{\omega}_{\alpha\gamma}(k) . \tag{2.11}$$

Equations (2.8) together with the closure in Eq. (2.7) make up a single nonlinear integral equation for $g(r) = 1 + h(r)$. It can be seen that all pair correlation information about the chemical structure of the polymer enters the theory through $\hat{\omega}(k)$. An important and unique feature of the PRISM theory that should be emphasized is that one has the ability to account for the effect of both local and global structural details, through $\hat{\omega}(k)$, on the intermolecular packing and thermodynamic properties of polymer liquids.

3 Intermolecular Packing in Homopolymer Melts

In PRISM theory the intramolecular architecture of the polymer is specified through $\hat{\omega}(k)$. The level of detail needed in the $\hat{\omega}(k)$ calculation depends on the particular question that one is addressing. For example, if one is interested in long range, universal aspects, a Gaussian model, in which the monomers are heavily coarse grained, would suffice. The effect of structural features like chain stiffness, operating on intermediate length scales, could be accounted for by

a semiflexible chain model. If one is interested in making detailed comparisons with experiment, the local monomeric structure details presumably must be included. In this section we give examples of PRISM calculations covering this range of detail.

3.1 Gaussian Chains

For chains consisting of sites connected by harmonic springs, the probability density between two intramolecular sites is a Gaussian distribution which can be written in Fourier transform space as

$$\hat{\omega}_{\alpha\gamma}(k) = \exp[-|\alpha - \gamma|k^2\sigma^2/6] \tag{3.1}$$

where σ is the statistical segment length. For simplicity we will take the statistical segment length equal to the hard core diameter d. The summation in Eq. (2.11) can easily be performed to yield

$$\hat{\omega}(k) = \frac{(1 - f^2 - 2f/N + 2f^{N+1}/N)}{(1 - f)^2} \tag{3.2}$$

where $f = \exp(-k^2\sigma^2/6)$. Equation (3.2) reduces to the well known Debye function in the limit of large N and $k\sigma \leqslant 1$. Then $\hat{\omega}(k)$ from Eq. (3.2) can be inserted into the generalized Ornstein-Zernike-like equation, Eq. (2.10) for the homopolymer, and the resulting equation can be solved numerically [11–15] subject to the Percus-Yevick hard sphere closure condition, Eq. (2.7). The numerical solutions were obtained using a variational method of Lowden and Chandler [9].

Results from this solution are shown for a melt of 2000 unit Gaussian chains in Fig. 1 as the points. Note that g(r) is a small number at contact ($r = \sigma = d$) and increases monotonically to unity on a scale of the radius of gyration R_g of the Gaussian chains. Such behavior is an example of the correlation hole predicted by deGennes [22]. The correlation hole is a consequence of the shielding of intermolecular interactions due to chain connectivity when two polymers are brought within R_g of each other. The "negative" correlation hole behavior (i.e., $g(r) < 1$) is a universal aspect of polymer melts and is a necessary consequence of chain connectivity and repulsive interactions between intermolecular segments. Note in Fig. 1 that the contact value of g(r) increases as the density increases at fixed chain length, reflecting the fact that the chain domains are pushed together as the density increases.

An analytical approximation [23] can be found for the Gaussian chain melt by taking either the so-called thread or string limits. The "thread-like chain" model has been discussed in depth elsewhere [23]. Mathematically, it corresponds to the limit that all microscopic length scales approach zero but their ratios remain finite. In particular, the site hard core diameter $d \to 0$, but the site density $\rho_m \to \infty$ such that the reduced density, $\rho_m d^3$, is non-zero and finite. In

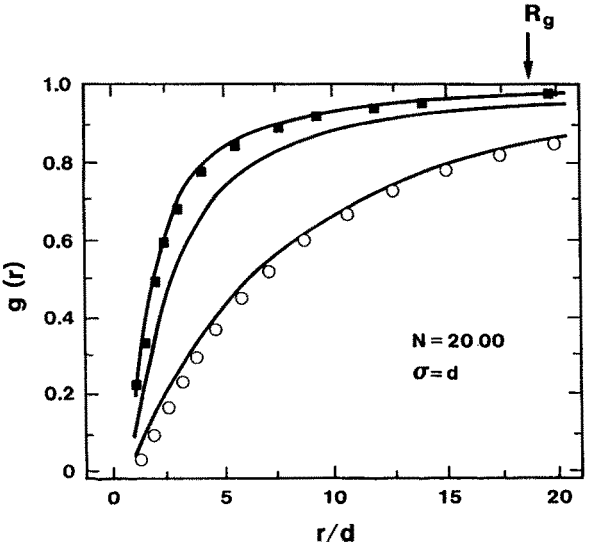

Fig. 1. Site-site intermolecular pair correlation function g(r) for 2000 unit Gaussian chains plotted as a function of reduced separation r/d. The solid curves are analytical results from the string model [23]. The *points* refer to the predictions from numerical solution of the PRISM theory for two reduced densities $\rho_m d^3$ of 0.2 (*open circles*) and 1.0 (*solid squares*). The *middle curve* is the analytical result for a reduced density of 0.6

the spirit of the Edwards' pseudopotential model[3a], the hard core direct correlation function is effectively replaced by a density-dependent delta-function. Hence the thread model does not represent the continuous $d \to 0$ limiting case of a finite range hard core repulsion. The latter model would have trivial ideal gas properties. Gaussian statistics are assumed to describe the single chain structure factor $\hat{\omega}(k)$, which is thus characterized solely by the statistical segment length σ, and the number of segments N. Moreover, in the thread limit the intramolecular structure factor can be accurately represented by the simple form[3a]: $\hat{\omega}(k) \cong [N^{-1} + (k\sigma)^2/12]^{-1}$.

With the above simplifications the PRISM equation can be analytically solved and yields [23] a site-site radial distribution of the Yukawa, or screened Coulomb, form:

$$g(r) = 1 + \frac{3}{\pi\rho_m\sigma^3} \frac{[\exp(-r/\xi_\rho) - \exp(-r/\xi_c)]}{r/\sigma} . \tag{3.3}$$

Note the presence of two screening lengths ξ_ρ and ξ_c. ξ_c is of macromolecular dimension and is simply related to the radius of gyration $\xi_c = R_g/\sqrt{2}$. ξ_ρ, on the other hand, is short range at high density and is determined from the core condition. Note also that at high densities there is a wide "intermediate" region of intersite separation, $\xi_\rho \ll r \ll \xi_c$, where power law correlations occur,

i.e. $-h(r) \propto (\sigma/r)$. In the thread limit the hard core diameter is shrunk to a point and the core condition in Eq. (2.7) is approximated as $g(r = 0) = 0$, for which ξ_ρ becomes [23]

$$\xi_\rho^{-1} = \xi_c^{-1} + \frac{\pi\rho_m\sigma^3}{3\sigma} \quad \text{(thread limit)} . \tag{3.4a}$$

A related model, the string model, takes the hard core d as finite, but the core condition is only satisfied on average, that is

$$\int_0^d r^2 g(r) dr = 0 .$$

This condition can be justified as an optimized perturbative treatment of the $d \neq 0$ polymer using the thread as a reference system [23]. In this case ξ_ρ is given by the transcendental equation

$$\frac{\xi_\rho}{\sigma}\left(\frac{\xi_\rho}{\sigma} + \Gamma^{-1}\right)\exp(-\sigma/\xi_\rho\Gamma) - \left(\frac{\xi_\rho}{\sigma}\right)^2 = \frac{\pi\rho_m d^3}{9} - \left(\frac{\xi_c}{\sigma}\right)^2 + \frac{\xi_c}{\sigma}\left(\frac{\xi_c}{\sigma} + \Gamma^{-1}\right)\exp(-\sigma/\xi_c\Gamma) \quad \text{(string limit)} \tag{3.4b}$$

where $\Gamma = \sigma/d$ is the aspect ratio of the chain.

The analytical predictions from Eq. (3.3) in the string limit are shown as the solid curves in Fig. 1. It can be seen that the analytical approximation shows a remarkable agreement with the corresponding exact numerical PRISM calculations for a finite hard core diameter. Implicit to the thread or string approach is a coarse-graining of molecular structure over the segmental length scale. Hence, local chemical information is lost (except in an average manner) and detailed structural features such as oscillatory g(r) functions indicative of local solvation shells due to the non-zero space-filling volume of real monomers are not captured. However, the thread idealization does yield analytical results which for many systems and properties are in excellent qualitative, or semi-quantitative, agreement with numerical PRISM predictions for more realistic non-thread polymer models. This achievement is the primary reason for constructing and studying the thread and string models.

3.2 Semiflexible Chains

More realism can be introduced into the intramolecular calculation of $\hat{\omega}(k)$ by the freely jointed chain model in which the chains are made up of rigid bonds connected by freely rotating joints. In this model $\hat{\omega}(k)$ is given by Eq. (3.2) with $f(k) = \sin(k\sigma)/k\sigma$ where σ represents both the bond length and hard core diameter for the model of present interest. Because of the rigid bond nature of

the model, an additional short range structure is superimposed on the long range correlation hole aspect of g(r) that is not generally evident in Gaussian chains at the same density [14, 15]. Although the freely jointed chain model includes the constant bond length constraint similar to the very stiff chemical bonds present in real polymers, it assumes the chain is completely flexible and thus neglects local stiffness and short range excluded volume which are important features of real polymers.

The exact intramolecular distribution function for a semiflexible chain characterized by a local bond bending energy $\varepsilon_b(1 + \cos\theta)$ cannot be computed analytically. A convenient approximation, however, is given by the Koyama distribution [24, 25]

$$\hat{\omega}_{\alpha\gamma}(k) = \frac{\sin(B_{\alpha\gamma}k)}{B_{\alpha\gamma}k} \exp(-A^2_{\alpha\gamma}k) \tag{3.5}$$

where

$$A^2_{\alpha\gamma} = \langle r^2_{\alpha\gamma}\rangle(1 - C_{\alpha\gamma})/6$$

$$B^2_{\alpha\gamma} = C\langle r^2_{\alpha\gamma}\rangle$$

$$C^2_{\alpha\gamma} = \frac{1}{2}\left[5 - 3\frac{\langle r^4_{\alpha\gamma}\rangle}{\langle r^2_{\alpha\gamma}\rangle^2}\right].$$

Equation (3.5) can be shown to preserve the correct second $\langle r^2_{\alpha\gamma}\rangle$ and fourth $\langle r^4_{\alpha\gamma}\rangle$ moments of the intramolecular separation $r_{\alpha\gamma}$. Thus for a semiflexible chain of specified stiffness (through the second and fourth moments) the intramolecular structure function $\hat{\omega}(k)$ can be computed numerically from Eqs. (3.5) and (2.11). The second and fourth moments have been calculated by Honnell et al. [24] for the discrete version of the *wormlike chain* model of Porod from a knowledge of the chain stiffness parameters $\langle\cos\theta\rangle$ and $\langle\cos^2\theta\rangle$. The persistence length ξ of the chain is given by

$$\xi = \frac{\ell}{1 + \langle\cos\theta\rangle} \tag{3.6}$$

where ℓ is the bond length and θ is the bond angle. The semiflexible, wormlike chain is thus completely characterized by two parameters ξ (or equivalently the reduced bond bending energy $\beta\varepsilon_b$) and N. Another, more realistic alternative, is to employ the standard rotational isomeric state model [16] for the required moments. From a knowledge of the bond length and angle, and the rotational states and potentials, the rotational isomeric state model can be used to compute the moments $\langle r^2_{\alpha\gamma}\rangle$ and $\langle r^4_{\alpha\gamma}\rangle$, although calculation of the fourth moment is tedious.

An example [24] of the effect of chain stiffness on the radial distribution function can be seen in Fig. 2. In Fig. 2a, g(r) is plotted for a completely flexible,

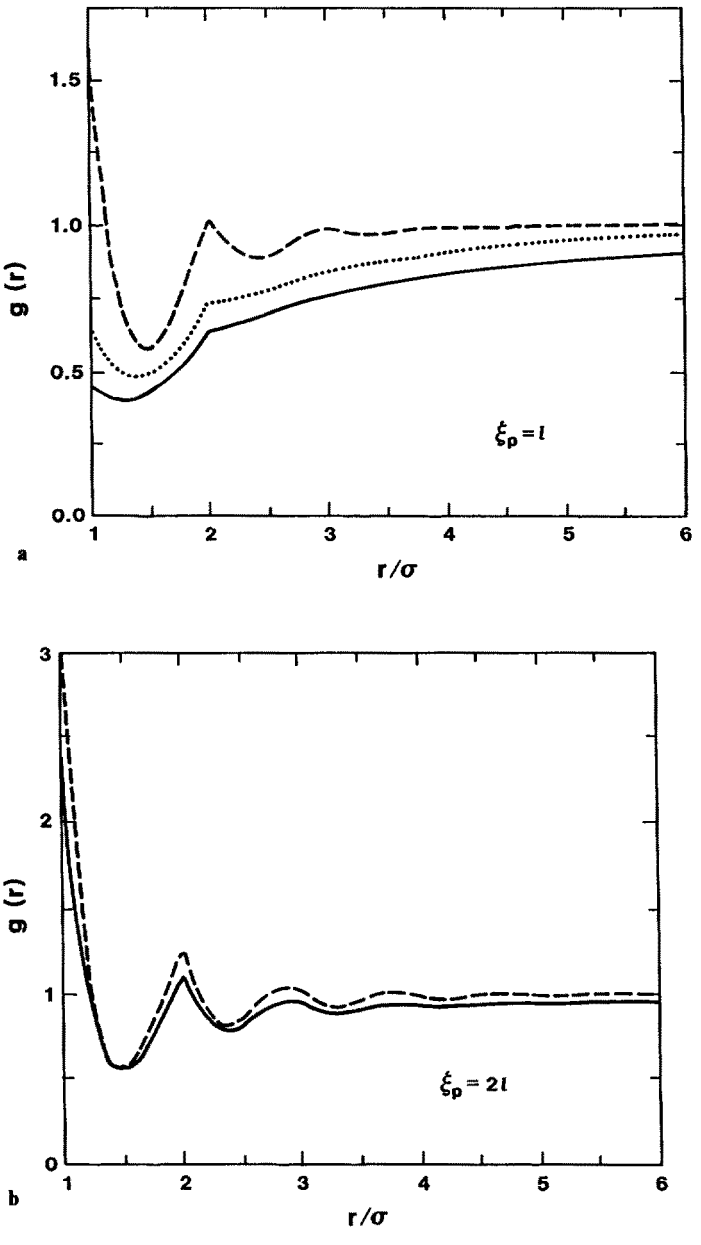

Fig. 2. a Intermolecular site-site radial distribution function g(r) for tangent hard core, freely jointed chains for a packing fraction $\eta = 0.5$ at three different chain lengths: N = 20 (*dashed*), N = 200 (*dotted*), N = 2000 (*solid*). The persistence length, $\xi = 1 = \sigma$, where 1 is the bond length and σ the hard core diameter. **b** Intermolecular site-site radial distribution function g(r) for tangent hard core, semiflexible chains [24] for a packing fraction $\eta = 0.5$ at two different chain lengths: N = 20 (*dashed*), and N = 2000 (*solid*). The persistence length is $\xi = 21$, where 1 is the bond length which equals the hard core diameter σ

freely jointed chain ($\xi = 1$) for several chain lengths N. Figure 2b shows the same plot for semiflexible chains having a persistence length $\xi = 2\ell$ and the "tangent" bead model is employed, i.e. $\ell = \sigma = d$. It can be seen that the contact value of g(r) increases significantly for the stiff chains. This increase in contact value and solvation shell structure results from the fact that the chains are expanded and thus pack more efficiently. Furthermore the chain length dependence of g(r) on local length scales is significantly reduced in the stiff chain case. The predicted results become virtually insensitive to increasing chain stiffness when $\xi \geqslant 4\ell$.

As an important caveat to the above results we note that PRISM theory does not deal accurately with longer range angular, or orientational correlations [26]. Thus, the description of strong, nematic-like local and/or global order is not generally possible. A generalization of the molecular integral equation approach to treat orientational correlations has been proposed by Chandler and co-workers [26] but the utility of this approach for chain molecules and polymers remains unexplored.

In order to test the quantitative validity of the PRISM predictions for homopolymer melts, we made detailed comparisons [24, 27] with the recent molecular dynamics simulations of Grest and Kremer. The simulations were performed on chains of length ranging from $N = 50$ to 200 at a liquid-like packing fraction of 0.464. The latter number has been determined from the relation $\eta = \pi\rho_m d^3/6$, where d is the effective hard core diameter discussed below. The repeat units interacted with a repulsive Lennard-Jones potential with $\beta\varepsilon = 1.0$. The simulation results are shown in Fig. 3 along with our PRISM predictions. The radial distribution functions of the Lennard-Jones soft core system were mapped onto an equivalent hard core problem using the standard Weeks, Chandler, Andersen (WCA) method [5, 27, 28]. If g(r) is computed using a freely jointed chain model it can be seen from Fig. 3 that the long correlation hole regime is accurately predicted, but the short range structure is underestimated.

Close examination of the radii of gyration from the molecular dynamics simulations reveals that the chains are not completely ideal. Overall the chains exhibit nearly ideal scaling behavior for which $R_g \propto N^{1/2}$. Locally, however, the chains are found to be expanded relative to a freely jointed chain of the same length. This local expansion is a result of local intramolecular excluded volume which has not been completely screened out in the melt. Thus in order to predict accurately the intermolecular structure one needs to correct for local deviations from Flory's ideality hypothesis. We were able to make this correction by employing the $\hat{\omega}(k)$ directly computed from the molecular dynamics simulation. When the PRISM theory is then used to calculate g(r) from the actual, simulated $\hat{\omega}(k)$, excellent agreement is seen in Fig. 3 between the theory and the simulation [27]. This agreement suggests that the PRISM theory can predict intermolecular structure with about the same accuracy as corresponding RISM calculations on small, rigid molecules. If only the radius of gyration, or mean square end-to-end distance, is available from simulation, an approximation can be made by using the semiflexible chain model in Eq. (3.5) where the persistence

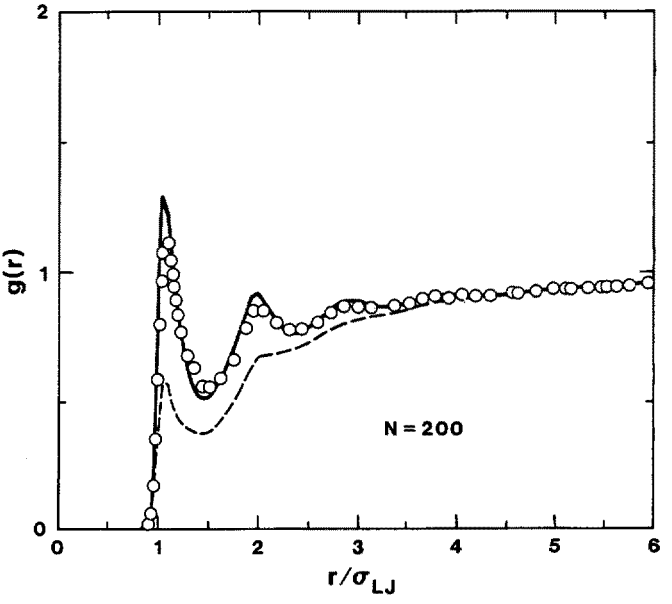

Fig. 3. Site-averaged intermolecular radial distribution function g(r) for N = 200. The *points* are the MD simulation of Kremer and Grest [27] (some points omitted for clarity). The *solid line* is the predicted result from the PRISM theory [27] using the simulated intramolecular $\hat{\omega}(k)$. The *dashed line* is the corresponding PRISM prediction using $\hat{\omega}(k)$ from a freely jointed chain model (with overlaps explicitly removed [14]). R_g is approximately 7.7 σ_{LJ} for the simulated chains

length is chosen to match the radius of gyration from simulation. Using this model intramolecular structure to compute g(r) also led to excellent agreement with the molecular dynamics simulations [24].

As the polymer fluid density decreases the agreement between PRISM and simulations becomes quantitatively poorer, even if the simulated $\hat{\omega}(k)$ is used in the PRISM calculation [29, 30]. Such a reduction of quantitative accuracy of the RISM approach also occurs for small, rigid molecule fluids and is a well-understood and documented trend [6].

3.3 Rotational Isomeric State Chains

The coarse grained models we have considered thus far are valuable for examining qualitative trends. However, in order to make comparisons directly with experimental data, more local structural details presumably need to be taken into account in the calculation of $\hat{\omega}(k)$. A realistic way of incorporating monomer structure is through the rotational isomeric state approximation, successfully employed [16] by Flory and others to describe isolated polymer chains in a theta solvent. In this description the continuous rotational potentials are replaced by discrete rotational states corresponding to the lowest vibrational

state in the potential wells. Short range excluded volume resulting from rotational correlations between adjacent bonds (pentane effect) is routinely incorporated into the calculations. Lower order moments of the end-to-end distance can be computed for this model but the complete distribution function necessary for determining $\hat{\omega}(k)$ cannot be explicitly obtained. An expansion of $\omega(r)$ in terms of the moments of the distribution is possible, but unfortunately the convergence is very slow [16].

An alternative approach is to generate $\hat{\omega}(k)$ through a single chain, Monte Carlo simulation by evaluating the average

$$\hat{\omega}(k) = \frac{1}{N}\left\langle \sum_{\alpha,\gamma=1}^{N} \frac{\sin(kr_{\alpha\gamma})}{kr_{\alpha\gamma}} \right\rangle . \tag{3.7}$$

An example of such a simulation [31] for a polyethylene chain of 1001 repeat units is shown as a Kratky plot in Fig. 4. This result for a single chain could then be introduced into Eq. (3.10) to compute the interchain packing from the PRISM theory.

A convenient and quite accurate alternative to computer simulation has been developed by McCoy et al. [31]. Here $\hat{\omega}(k)$ is computed as an approximation by including the structural detail only on short length scales. This is accomplished by rewriting $\hat{\omega}(k)$ in the form

$$\hat{\omega}(k) = \frac{1}{N}\sum_{\alpha}\left[\sum_{|\alpha-\beta|\leqslant 5} \hat{\omega}_{\alpha\beta}(k) + \sum_{|\alpha-\beta|>5} \hat{\omega}_{\alpha\beta}(k) \right] . \tag{3.8}$$

The first term for $|\alpha - \beta| \leqslant 5$ is evaluated by direct enumeration of rotational isomeric states, thereby including the pentane effect (longer range enumerations

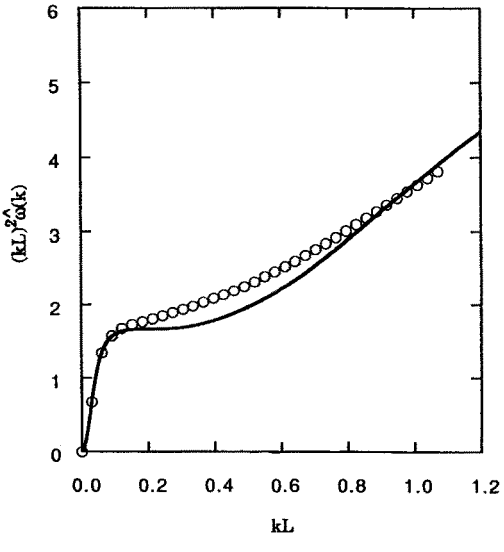

Fig. 4. A Kratky plot for a 1001 site rotational isomeric state polyethylene chain. The *circles* are from a Monte Carlo simulation [31] and the *curve* is the corresponding result using the approximate procedure described in the text. L is the carbon-carbon bond length

are also feasible). The long range contribution for $|\alpha - \beta| > 5$ is approximated by "splicing" on the Koyama distribution for a semiflexible chain [24, 25], where the second and fourth moments $\langle r^2_{\alpha\gamma} \rangle$ and $\langle r^4_{\alpha\gamma} \rangle$ are adjusted for each $|\alpha - \gamma|$ to match the corresponding moments from a rotational isomeric state computation. This approximate calculation is also shown in Fig. 4. The standard alkane rotational isomeric state parameters were used in both the Monte Carlo and the approximate calculation (bond length $\ell = 1.54$ Å, bond angles $\theta = 112°$, gauche states at $\phi = \pm 120°$, with energy of 500 cal/mol relative to trans, and 2000 cal/mol for the g^+g^- state) [16]. It is interesting to note that the approximate procedure yields a well defined intermediate scaling regime indicated by the plateau on the Kratky plot; no corresponding intermediate scaling regime is found for the Monte Carlo calculation. This issue and its experimental and theoretical implications are discussed in depth by McCoy and co-workers [31].

Honnell et al. computed [32, 33] the intermolecular packing correlations for a polyethylene melt (N = 6429) at 430 K from the PRISM theory using the above approximate procedure. The results for the structure factor are shown in Fig. 5. The static structure factor is defined as

$$\hat{S}(k) = \hat{\omega}(k) + \rho_m \hat{h}(k) \tag{3.9}$$

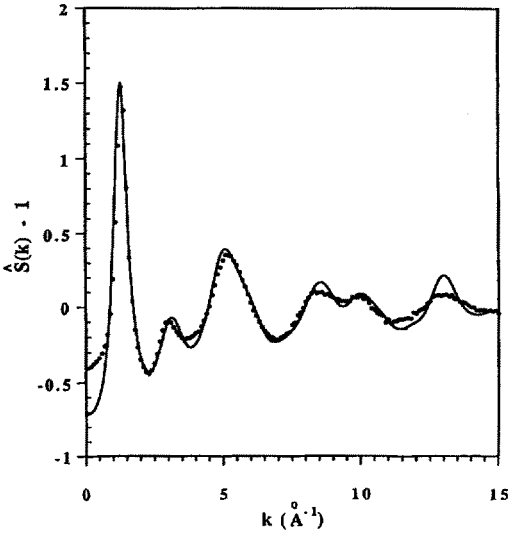

Fig. 5. Structure factor $\hat{S}(k)$ for polyethylene melt (N = 6429) as a function of wavevector k at T = 430 K. The *points* are experimental results [32, 33] of Narten and Habenschuss from X-ray scattering (the $k \approx 0$ data is inaccurate due to sample preparation related scattering). The *solid curve* is the PRISM theory with the hard core diameter d = 3.90 Å. Use of a value of d = 3.7 Å results in roughly a 10% underestimate of the intensity of the amorphous halo feature. Disagreement between experiment and theory at large k is eliminated if thermal broadening, due to vibrational and torsional oscillations, is taken into account [33, 34]

and represents the Fourier transform of the total density fluctuation correlation function. The methylene groups along the chain were represented by overlapping hard sphere sites of diameter d. Also shown in this figure is the structure factor from experimental X-ray scattering measurements [32, 33] on the same polyethylene melt by Narten and Habenschuss. The hard core diameter d, adjusted in the PRISM theory to match the height of the first peak in the experimental $\hat{S}(k)$ curve, yielded a value of 3.90 Å. This is a very reasonable value [32] based on crystalline-packing-based geometrical estimates for the volume of a CH_2 unit. It can be seen from Fig. 5 that the agreement between the PRISM theory and X-ray scattering experiment is quite satisfactory. Analysis of the intramolecular and intermolecular contributions to the structure factor in Eq. (3.9) indicates that for $k > 6$ Å^{-1}, $\hat{S}(k)$ is almost entirely intramolecular in origin. The contributions to $\hat{S}(k)$ for $k < 6$ Å^{-1} are due to both intra- and intermolecular correlations. It is important to mention that good agreement with experiment was found even though we used hard core interactions between sites, and did not include attractions. This is not surprising since it is well known [5, 6] that the intermolecular radial distribution function and wide angle diffraction pattern are primarily controlled by repulsive interactions at high density. On the other hand, $\hat{S}(k = 0)$ is a thermodynamic property which is very sensitive to attractive interactions, and is generally not as accurately predicted by the RISM approach. Systematic PRISM calculations for the alkane series have also been carried out by Honnell et al. and compared with X-ray scattering measurements [34]. Agreement between theory and experiment is comparable to the polyethylene case.

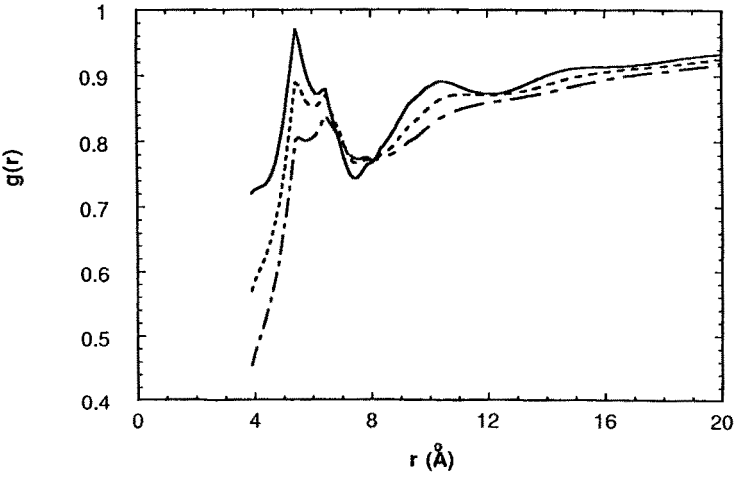

Fig. 6. Intermolecular radial distribution function g(r) computed for polyethylene (d = 3.90 Å, T = 430 K, N = 6429) using PRISM theory. $\rho_m d^3 = 2.2$ (*solid curve*), 2.0 (*short dashed*), 1.8 (*dash-dot*). At one atmosphere pressure the experimental value of $\rho_m d^3$ is ~ 2.0

Figure 6 shows our PRISM theory predictions for g(r) of polyethylene at 430 K and three different densities using d = 3.90 Å for the hard core diameter. Note that g(r) for polyethylene is somewhat more complex than in the tangent hard sphere calculations in Figs. 2 due to the multiplicity of length scales (i.e. $d \neq \ell \neq \xi$). The first peak, which occurs at the hard core diameter for tangent hard spheres, is shifted out to $d + \ell$. The cusps that occur in g(r) arise because of the hard sphere and constant bond length constraints [6]. The correlation hole regime is also clearly evident beyond roughly 15–20 Å in which g(r) approaches unity on a scale of the radius of gyration ($R_g \sim 130$ Å) in a power law manner.

4 Equation-of-State

Based on comparison with Monte Carlo simulations in Fig. 3 and X-ray scattering experiments in Fig. 5, it would seem that PRISM theory is accurate for the intermolecular structure in polymer melts. Given the site-site radial distribution function g(r) it should, in principle, be possible to deduce the equation-of-state and other thermodynamic properties. Unlike g(r), which is sensitive only to the repulsive branch of the potential, one expects that the equation-of-state will also be a function of the range and magnitude of the attractions. The fact that g(r) is primarily controlled by repulsions at high density suggests that the effect of attractions on the pressure can be treated by perturbation theory [5, 6, 28, 35] about a hard core reference system. Such an expansion should be particularly valid at high temperatures or small $\beta\varepsilon$, where ε is the attractive interaction energy scale of, for example, a Lennard-Jones potential,

$$v(r) = 4\varepsilon[(\sigma_{LJ}/r)^{12} - (\sigma_{LJ}/r)^{6}] \,. \tag{4.1}$$

The effective hard core is optimally chosen such that a selected property of the continuous repulsive force fluid is accurately reproduced by the hard core reference system [5, 6, 28, 35].

In the Barker-Henderson [5, 35] perturbation theory the potential in Eq. (4.1) is divided into a repulsive branch $v_0(r)$ and an attractive branch $v_a(r)$

$$\begin{aligned} v_0(r) &= v(r); \quad r \leqslant \sigma_{LJ} \\ &= 0; \quad\quad r > \sigma_{LJ} \\ v_a(r) &= 0; \quad\quad r \leqslant \sigma_{LJ} \\ &= v(r) \quad r > \sigma_{LJ} \,. \end{aligned} \tag{4.2}$$

The optimum hard core diameter is then given by

$$d = \int_0^\infty \{1 - \exp[-\beta v_0(r)]\} dr \,. \tag{4.3}$$

Similarly in the perturbation theory of Weeks, Chandler and Andersen [5, 28] (WCA) the Lennard-Jones potential is decomposed according to

$$\begin{aligned} v_0(r) &= v(r) + \varepsilon, \quad r \leqslant 2^{1/6}\sigma_{LJ} \\ &= 0, \qquad\quad r > 2^{1/6}\sigma_{LJ} \\ v_a(r) &= \quad -\varepsilon, \quad r \leqslant 2^{1/6}\sigma_{LJ} \\ &= v(r), \qquad r > 2^{1/6}\sigma_{LJ} \,. \end{aligned} \tag{4.4}$$

Here the optimum hard core diameter d is chosen to satisfy

$$\int_0^d r^2 \exp[-\beta v_0(r)] C_0(r;d)dr + \int_d^\infty r^2 \{1 - \exp[-\beta v_0(r)]\} g_0(r;d)dr = 0 \tag{4.5}$$

where C_0 and g_0 are the direct correlation function and radial distribution function, respectively, for the hard core reference system subject to the PY closure in Eq. (2.7).

Given a knowledge of $g_0(r)$, the pressure of the optimized hard core polymer liquid can be computed in several ways. The simplest route is merely to integrate the isothermal compressibility [5, 6] κ_T which is related to the zero wavelength structure factor $\rho_m k_B T \kappa_T = \hat{S}(0)$:

$$\frac{\beta P}{\rho_m} = \frac{1}{\rho_m} \int_0^{\rho_m} \hat{S}^{-1}(0, \rho_m')d\rho_m' \,. \tag{4.6}$$

$\hat{S}(0)$ involves all length scales and presumably is relatively more sensitive to the long range part of $g_0(r)$. Another route to the pressure is through the Helmholtz free energy A. The free energy of a hard core system can be computed according to a "charging formula" given by [6]

$$\frac{A - A_0}{V} = 2\pi\rho_m^2 d^3 k_B T \int_0^1 g^{(\lambda)}(\lambda d^+)\lambda^2 d\lambda \tag{4.7}$$

where the hard core diameter is gradually "turned on" as λ varies from 0 to 1. In Eq. (4.7), $g^{(\lambda)}(\lambda d^+)$ is the contact value of g(r) for a liquid comprised of interaction sites of diameter λd and A_0 is the free energy of an ideal gas. The pressure is then obtained from Eq. (4.7) by numerical differentiation with respect to volume. In the case of a simple hard sphere fluid, Eq. (4.7) can be shown [6] to reduce to the well known virial formula. For molecular fluids, however, one must explicitly carry out the integration over λ. Since the integrated quantity in Eq. (4.7) is the site-site radial distribution function at contact, the free energy route to the pressure is sensitive to the very short range character of the intermolecular packing. A third route to the pressure makes use of $g_w(r)$, the wall-fluid distribution function

$$\frac{\beta P}{\rho_m} = g_w(0) \,. \tag{4.8}$$

The quantity $\rho_m g_w(0)$ is the density of molecular sites in contact with a hard wall. This method was employed recently by Dickman and Hall [36] to determine pressure from Monte Carlo simulations. Yethiraj and Hall [37] demonstrated that $g_w(r)$ can be approximately computed from PRISM theory by considering a mixture of polymer chains and spherical particles in the limit of zero concentration of particles with diameters approaching infinity.

If $g_0(r)$, $g^{(\lambda)}(r)$, and $g_w(r)$ are known exactly, then all three routes should yield the same pressure. Since liquid state integral equation theories are approximate descriptions of pair correlation functions, and not of the effective Hamiltonian or partition function, it is well known that they are thermodynamically inconsistent [5]. This is understandable since each route is sensitive to different parts of the radial distribution function. In particular, g(r) in polymer fluids is controlled at large distance by the correlation hole which scales with the radius of gyration or $\sqrt{N}$. Thus it is perhaps surprising that the hard core equation-of-state computed from PRISM theory was recently found by Yethiraj et al. [38, 39] to become more thermodynamically inconsistent as N increases from the diatomic to polyethylene. The uncertainty in the pressure is manifested in Fig. 7 where the insert shows the equation-of-state of polyethylene computed [38] from PRISM theory for hard core interactions between sites. In this calculation, the hard core diameter d was fixed at 3.90 Å in order to maintain agreement with the experimental structure factor in Fig. 5.

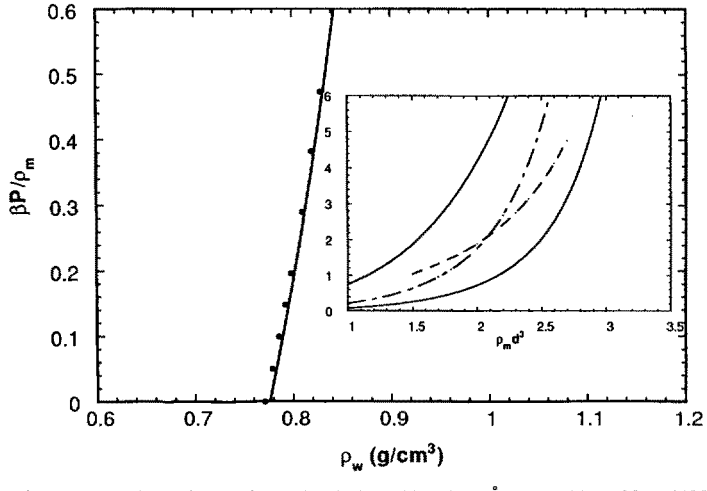

Fig. 7. Equation-of-state for polyethylene (d = 3.90 Å, T = 430 K, N = 6429). The *solid curve* was computed from the GFD hard sphere reference system [38] with the effect of attractions computed by Barker-Henderson perturbation theory [35] using g(r) obtained from PRISM theory. The points are experimental PVT data of Olabisi and Simha [41]. The *inset* shows the hard sphere equation-of-state computed by various routes: free energy (*upper solid*), compressibility (*lower solid*), wall (*dashed*) GFD (*long-dash-dot*).

It is difficult to assess the accuracy of the pressure obtained from the three routes since computer simulations of polyethylene hard core chains have not yet been performed at high density. In Fig. 7 we have also plotted the pressure predicted from a continuous space mean field equation-of-state, the generalized Flory dimer model [40] (GFD), appropriately generalized by Yethiraj et al. [38] to treat the overlapping site rotational isomeric state model. Prior detailed comparisons between the GFD predictions and off-lattice computer simulations suggest this equation-of-state is accurate for long chains at high density. It can be seen from the inset in Fig. 7 that the GFD equation-of-state is bounded by the compressibility and free energy routes. The wall route is reasonably close to the GFD result, but the isothermal compressibility is predicted to be too high.

The pressure of a realistic polymer liquid interacting with Lennard-Jones potential can now be approximated from the hard core reference system using thermodynamic perturbation theory:

$$A \cong A_{HS} + \tfrac{1}{2}\rho_m^2 \int g_0(r) v_a(r) d\vec{r} \,. \tag{4.9}$$

In Eq. (4.9) A_{HS} is the Helmholtz free energy of the hard core reference system with the optimized hard core diameter. The pressure of the full system can be found from Eq. (4.9) by differentiation with respect to volume. This pressure will be a function of the two Lennard-Jones parameters σ_{LJ} and ε.

In the case of polyethylene, we observed in the previous section that to be consistent with the experimental structure factor the hard core diameter should be fixed at d = 3.90 Å at 430 K. With this added constraint we therefore have only a single adjustable parameter since d is related to σ_{LJ} and ε through the Barker-Henderson relation, Eq. (4.3) or WCA equation, Eq. (4.5).

The equation-of-state of polyethylene at 430 K has been calculated [38, 39] using the above procedure with the three routes to the hard core reference liquid in Eqs. (4.6)–(4.8). Of these three reference systems, the "wall route" in Eq. (4.7) gave the best agreement with experimental PVT data. Better agreement with experiment could be obtained, however, by using the appropriately modified GFD approach [38] for the pressure of the hard core reference system. The pressure of the system with the full Lennard-Jones potential was then computed from Eq. (4.9) with the radial distribution function $g_0(r)$ obtained from PRISM theory. The results of this hybrid calculation for polyethylene are shown in Fig. 7 along with the experimental PVT data of Olabisi and Simha [41]. Using the Barker-Henderson relation in Eq. (4.3) to maintain the constraint of d = 3.90 Å, the values of σ_{LJ} = 4.36 Å and ε/k_B = 38.7 K gave good agreement with the experimental PVT data as can be seen in Fig. 7. This particular set of Lennard-Jones parameters is consistent with the recent Monte Carlo study of Lopez-Rodriguez and coworkers [42] on the second virial coefficients of hydrocarbon fluids.

The above considerations suggest that the hard core radial distribution function obtained for polyethylene was sufficiently accurate on short length scales to predict the perturbative contribution (Eq. (4.9)) to the attractive branch

of the potential. The difficulty lies in computing the pressure of the hard core reference system. It is clear from the inset in Fig. 7 that there is a large uncertainty in the hard core pressure due to the thermodynamic inconsistency among the different routes. It is likely that this problem can be improved by using methods developed [5] for obtaining thermodynamically consistent results for atomic and small molecule fluids. Following these ideas, one adds a nonzero tail of some assumed functional form to the direct correlation function outside the hard core. The parameters in this function are then chosen in such a way as to force thermodynamic consistency constraints [43].

5 Polymer Crystallization

A number of years ago Flory developed [44] a mean field incompressible lattice model to describe the equilibrium freezing of polymers. Although the model has the virtue of simplicity, it suffers from at least three well known deficiencies. (1) It is an incompressible model that does not account for the density change associated with the first order freezing transition. This density change is not negligible for many polymers, for example, polyethylene exhibits approximately a 30% densification on crystallization from the melt. (2) Attractive intermolecular forces are ignored. (3) The Flory approach is a mean field theory that neglects intra- and intermolecular correlations. Nagle et al. [45] have argued that such approximations, plus the unrealistic nature of packing on a lattice, seriously affect the validity of the Flory crystallization theory.

More recently, density functional theory has been successfully applied to the freezing of monatomic [46, 47] and polyatomic [48–51] liquids. In a common application of density functional theory to freezing, the excess free energy of the solid is expanded about the structure of the liquid at density ρ_L. The free energy functional is customarily truncated at second order in the order parameter $\Delta\rho(r) = \rho(r) - \rho_L$ where $\rho(r)$ is the nonuniform, single particle density of the solid phase. It has been found that the errors introduced from the higher order terms can be compensated for, to some degree, by expanding the free energy difference between the system of interest and some ideal system which can be solved exactly. In this manner the higher order terms in the expansion of the ideal and true system tend to cancel, thereby providing a more accurate density functional.

McCoy and coworkers [52] have generalized this density functional scheme to describe the crystallization of polymers. In this approach the structure of the liquid is provided by PRISM theory. Three conditions are necessary in order to ensure equilibrium between the solid and liquid phases. (1) temperature equality, (2) equality of the chemical potentials μ, and (3) pressure equality. Because of these conditions it is more convenient to work with the Grand potential W rather than the more conventional Helmholtz free energy A. W is related to

A through a Legendre transform

$$W = A - \sum_i \int d\vec{r} \psi_i(\vec{r}) \rho_i(\vec{r}) \tag{5.1}$$

where $\rho_i(\vec{r})$ is the density of sites of type i. In density functional theory it is envisaged that an external field $\psi_i(\vec{r})$ acts on sites of type i to give the non-uniform density profile $\rho_i(\vec{r})$. The Grand potential difference ΔW between the solid and liquid phase is defined as

$$\Delta W = W[T, V, \mu, \rho_i(\vec{r})] - W[T, V, \mu, \rho_L] \tag{5.2}$$

where μ is the chemical potential. Introducing an ideal system denoted by superscripts "o" and using PRISM theory for the structure of the liquid phase, the Grand potential functional ΔW can be written as [52]

$$\begin{aligned} \Delta W = & \sum_i \int d\vec{r} [\psi_{L,i} - \psi_i(r)] \rho_i(\vec{r}) + \sum_i \int d\vec{r} [\psi_i^o(r) - \psi_{L,i}^o] \rho_i(\vec{r}) \\ & - \frac{1}{N} \sum_i \int d\vec{r} \Delta\rho_i(\vec{r}) - \frac{1}{2} \sum_{i,j} \iint d\vec{r} d\vec{r}' C_{ij}(\vec{r} - \vec{r}') \Delta\rho_i(\vec{r}) \Delta\rho_j(\vec{r}') \\ & + \cdots \end{aligned} \tag{5.3}$$

where $\psi_i(r)$ and $\psi_i^o(r)$ refer to the position dependent external fields for the real and ideal solid, and $\psi_{L,i}$ and $\psi_{L,i}^o$ are the constant external fields for the uniform real and ideal liquid phases. $C_{ij}(r)$ is the direct correlation function between sites i and j and is to be determined from PRISM theory.

A convenient ideal system for the liquid phase is a collection of chains each of which is described by the rotational isomeric state model [16]. For such a system we can write the external field $\psi_{L,i}^o$ as

$$\psi_{L,i}^o = \frac{1}{N} \ln\left(\frac{1}{N}\right) \sum_i \rho_{L,i} - \frac{(N-1)}{N} \ln\lambda \tag{5.4a}$$

where λ is determined [16] from the rotational isomeric state theory as

$$\lambda = \tfrac{1}{2}\{1 + s(1 + w) + \sqrt{[1 - s(1 + w)]^2 + 8s}\} \tag{5.4b}$$

and s and w are simply related to the gauche energy E_g and gauche$^+$gauche$^-$ energy E_{g+g-}:

$$s = \exp(-E_g/RT); \quad w = \exp(-E_{g+g-}/RT)\,. \tag{5.4c}$$

For simplicity, torsional and other vibrations of the ideal crystalline solid are ignored, and it is assumed that the chains are in the all-trans configuration. In this case the ideal external field of the solid has the form

$$\psi^o = \frac{1}{N} \ln\left(\frac{1}{N}\right) \sum_i \rho_{L,i}\,. \tag{5.5}$$

For this ideal system, Eq. (5.3) can be simplified for the homopolymer case of identical sites to give [52]

$$\frac{\Delta W}{\rho_L V} = \int d\vec{r} \ln \lambda \rho(\vec{r}) - \tfrac{1}{2} \iint d\vec{r} d\vec{r}' C(|\vec{r} - \vec{r}'|) \Delta\rho(\vec{r}) \Delta\rho(\vec{r}') \,. \tag{5.6}$$

One proceeds numerically to minimize ΔW with respect to the liquid density ρ_L and a parametrized solid phase density profile $\rho(\vec{r})$. PRISM theory is used to compute the site-site direct correlation function C(r). This procedure is repeated with different assumed solid profiles until one finds the profile such that $\Delta W_{min} = 0$. It can be demonstrated that this profile corresponds to the coexistence curve where the three conditions for equilibrium between liquid and solid are satisfied. Such a program has been carried out to describe the freezing of polyethylene (PE) and polytetrafluoroethylene (PTFE) melts [52] and the results are depicted in Fig. 8. In this work the orthorhombic crystal was assumed to be the most stable ordered phase.

In Fig. 8 the predicted temperature-density behavior of coexisting liquid and solid phases are shown along with experimental data for PE [53] and PTFE [54]. Based on the experimental equation-of-state [41] the melting temperature T_m for PE is predicted to be 427 K, in good agreement with experiment (415–420 K). Excellent agreement is also found for the liquid density at the coexistence point and some of the lattice parameters [52]. For PTFE,

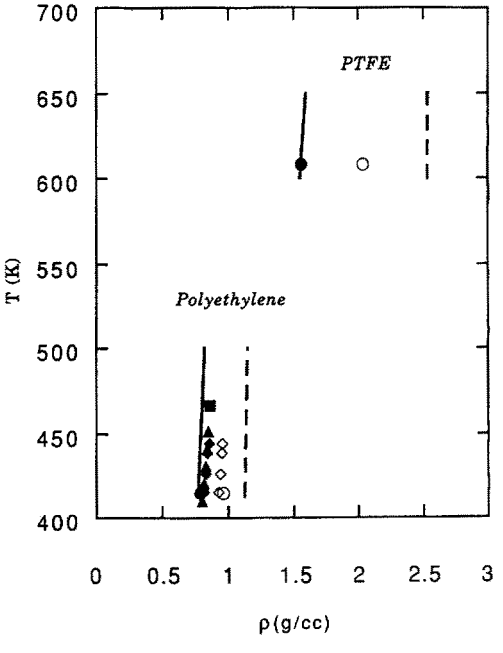

Fig. 8. Solid-liquid phase diagram for polyethylene (*lower*) and polytetrafluoroethylene (PTFE) (*upper*) computed from PRISM plus density functional theory [52]. The *solid* (*dashed*) *lines* are the theoretical liquid (solid) predictions. The *solid* (*open*) symbols are the experimental results [53, 54] for the coexistence of liquid (solid)

$T_m = 608$ K is predicted whereas the experimental values are given by 607 ± 10 K. Heuristic arguments suggest that PTFE should have a larger freezing temperature than PE because of the increased chain stiffness in PTFE. Following the Flory theory [44] of melting would imply that T_m/E_g should be approximately constant. Such reasoning would lead to the conclusion [52] that for PTFE, $T_m \sim 1000$ K, assuming that PE has a melting temperature of 420 K. Thus it appears that freezing of polymers is more subtle than a simple chain stiffness argument and presumably involves other factors such as chain packing and local chemical structure. It can also be observed from Fig. 8 that the predicted volume changes on crystallization from density functional theory are larger than observed experimentally. This trend is to be expected since it was assumed for calculation purposes that torsional oscillations, which would reduce the solid density, were not present. The removal of this simplification is certainly feasible and represents an important direction for future research.

From a more general perspective, the polymer density functional theory predicts that the location, or even existence, of a melting line is very sensitive to the Angstrom level chemical structure, volume change and attractive forces [52]. Neglect of any of these features can destroy the stability of the orthorhombic crystalline phase. For example, Gaussian and freely rotating chain models were found never to crystallize due to their excessive conformational entropy content in the disordered phase. Such behavior is consistent with the arguments of Nagle et al. [45], and the general understanding of a strongly first order phase transition as a highly nonuniversal process sensitive to many competing factors.

6 Polymer Blends: General Aspects

The structure and properties of phase-separating polymer alloys is a subject of considerable scientific and technological interest [55]. With the advent of the small angle neutron scattering (SANS) technique much information concerning concentration fluctuations in polymer alloys has been accumulated, and is commonly expressed in terms of an empirical "apparent chi-parameter", χ_s, which contains all non-ideal mixing information [56]. According to classical mean field Flory-Huggins ideas [1], the chi-parameter is a purely energetic quantity which is inversely proportional to temperature and completely determined by the local chemical interactions between monomers embedded in a structureless fluid. In practice, chi-parameters and phase diagrams of real polymer alloy materials are far more complex and exhibit a host of "non-mean field" features of both enthalpic and entropic origins. For example, χ_s often depends strongly on composition, local chain stiffness, pressure, global chain architecture, molecular weight, chain branching, and possibly wavevector of observation [57, 58]. The ability to understand the phase behavior of existing polymer mixtures, and ultimately to predict and control the miscibility of novel

alloys, requires new theoretical methods that can account for the multitude of correlation effects.

The PRISM integral equation theory has been generalized for multicomponent polymer mixtures by Curro and Schweizer [23, 59–63]. Much formally exact analysis can be carried out based simply on the structure of the PRISM matrix integral equations without specifying a particular closure approximation [61]. In this section these aspects are summarized.

6.1 PRISM Formalism

A standard interaction site model of homopolymers is adopted where the pairwise decomposable site-site intermolecular potentials consist of a hard core repulsion plus a more slowly spatially varying tail.

$$\begin{aligned} u_{MM'}(r) &= u^{(0)}_{MM'}(r) = \infty, \quad r < d_{MM'} \\ &= v_{MM'}(r), \quad r \geqslant d_{MM'} . \end{aligned} \tag{6.1}$$

Continuous repulsive potentials can easily be treated using the WCA perturbation approach [5, 6, 28] (see Eq. (4.5)) to map the problem of interest onto an effective hard core model. Generalization to the case of heteropolymers composed of more than one type of site is also straightforward. The PRISM matrix equations for the homopolymer mixture is given in Fourier-transform space by [59]

$$\hat{h}_{MM'}(k) = \hat{\omega}_M(k)\left[\hat{C}_{MM'}(k)\hat{\omega}_{M'}(k) + \sum_{M''} \hat{C}_{MM''}(k)\rho_{M''}\hat{h}_{M''M'}(k)\right] \tag{6.2}$$

where chain-end effects have been averaged over in the usual manner [13]. Here, ρ_M is the site number density of species M, $h_{MM'}(r) = g_{MM'}(r) - 1$, where $g_{MM'}(r)$ is the chain-averaged intermolecular pair correlation (or radial distribution) function between interaction sites of species M and M', $C_{MM'}(r)$ is the corresponding intermolecular site-site direct correlation function, and $\hat{\omega}_M(k)$ is the intramolecular structure factor of species M.

The partial density-density collective structure factors are given by

$$\hat{S}_{MM'}(k) = \rho_M\hat{\omega}_M(k)\delta_{M,M'} + \rho_M\rho_{M'}\hat{h}_{MM'}(k) \tag{6.3}$$

We concentrate here on a binary homopolymer blend under constant volume conditions; generalizations to ternary or more complex mixtures is straightforward. Substituting the PRISM Eq. (6.2) in Eq. (6.3) yields

$$\hat{S}_{AA}(k) = \rho_A\hat{\omega}_A(k)[1 - \rho_B\hat{\omega}_B(k)\hat{C}_{BB}(k)]/\Lambda(k) \tag{6.4a}$$

$$\hat{S}_{BB}(k) = \rho_B\hat{\omega}_B(k)[1 - \rho_A\hat{\omega}_A(k)\hat{C}_{AA}(k)]/\Lambda(k) \tag{6.4b}$$

$$\hat{S}_{AB}(k) = \rho_A\rho_B\hat{\omega}_A(k)\hat{\omega}_B(k)\hat{C}_{AB}(k)/\Lambda(k) \tag{6.4c}$$

$$\Lambda(k) = 1 - \rho_A \hat{\omega}_A(k)\hat{C}_{AA}(k) - \rho_B \hat{\omega}_B(k)\hat{C}_{BB}(k) + \rho_A \rho_B \hat{\omega}_A(k)\hat{\omega}_B(k) \times [\hat{C}_{AA}(k)\hat{C}_{BB}(k) - \hat{C}^2_{AB}(k)] \,. \tag{6.5}$$

The direct correlation functions contain the fundamental microscopic information regarding interactions and correlations in blends. In general there are three independent functions for a binary homopolymer mixture, which enter the scattering functions in a nonlinear fashion. On the relatively long length scales relevant to small angle scattering measurements the approximation $\hat{C}_{MM'}(k) \cong \hat{C}_{MM'}(0) \equiv C_{MM'}$ is appropriate. The spinodal condition is given by the simultaneous divergence at $k = 0$ of all the partial structure factors

$$0 = 1 - \rho_A N_A C_{AA} - \rho_B N_B C_{BB} + \rho_A \rho_B N_A N_B [C_{AA} C_{BB} - C^2_{AB}] \,. \tag{6.6}$$

The total density fluctuations are characterized by the isothermal compressibility, κ_T, which is given by [63, 64]:

$$\kappa_T^{-1} = k_B T \sum_{M,M'} \rho_M \rho_{M'} \hat{S}^{-1}_{MM'}(0)$$

$$= k_B T \left\{ \frac{\rho_A}{N_A} + \frac{\rho_B}{N_B} - [\rho_A^2 \hat{C}_{AA}(0) + \rho_B^2 \hat{C}_{BB}(0) + 2\rho_A \rho_B \hat{C}_{AB}(0)] \right\} \tag{6.7}$$

where N_M is the number of interaction sites comprising a molecule of species M. The inverse isothermal compressibility generally remains nonzero at the spinodal defined by Eq. (6.6), but will vanish at a liquid-gas-like transition. As recently emphasized in the simple liquid integral equation context [65], liquid-liquid phase separation is a coupled density and concentration fluctuation process and thus compressibility effects generally play an important role.

6.2 Connections with IRPA and SANS Chi-Parameter

The incompressible random phase approximation (IRPA) is routinely used by experimentalists to analyze small angle scattering data from polymer alloys. A common approach to empirically defining an apparent SANS chi-parameter, χ_S, is based on the total scattering intensity extrapolated to $k = 0$ as [56, 57]:

$$\frac{k_N}{\hat{S}_E(0)} \equiv \frac{\left(\frac{b_A}{V_A} - \frac{b_B}{V_B}\right)^2}{\sum_{M,M'} b_M b_{M'} \hat{S}_{MM'}(0)} = \frac{1}{\phi_A N_A V_A} + \frac{1}{\phi_B N_B V_B} - 2\frac{\chi_S}{V_0} \,. \tag{6.8}$$

Here, $\phi_M = \rho_M V_M/\eta$ is the volume fraction of sites of type M, V_M is the volume of a site of type M, V_0 is a "reference volume", and b_M is the total neutron scattering length of a site of species M. Note that this chi-parameter will generally diverge as $\phi_M \to 0$ due to the unrealistic incompressibility assumption. The SANS chi is, by construction, equivalent to the incompressible Flory value at the spinodal.

Substitution of Eq. (6.4) into Eq. (6.8) yields a general expression for the SANS chi-parameter which can be employed in PRISM studies to make direct contact with experiments on specific blends. Such an approach to comparing theory and experiment has been emphasized by Dudowicz, Freed, and coworkers [2] as the most appropriate procedure. The resultant empirical chi-parameter contains not only microscopic information concerning intermolecular interactions in blends (i.e. some combination of the independent $C_{MM'}$), but also reflects all the errors made by the neglect of compressibility effects which depend on N_M, T, ϕ_M, etc. [2].

The general, wavevector-dependent IRPA scattering function for pure concentration fluctuation scattering is given by [57, 61]

$$\hat{S}_c^{-1}(k) = r^{-1/2}[\phi_A \hat{\omega}_A(k)]^{-1} + r^{1/2}[\phi_B \hat{\omega}_B(k)]^{-1} - 2\hat{\chi}_s(k) \tag{6.9}$$

where $r = V_A/V_B$ and $\eta = \rho_A V_A + \rho_B V_B$ is the total site packing fraction. The corresponding IRPA spinodal condition is

$$2\chi_s = r^{-1/2}(N_A\phi_A)^{-1} + r^{1/2}(N_B(1-\phi_A))^{-1} . \tag{6.10}$$

Note that in the hypothetical incompressible limit the form of both the scattering functions and spinodal condition are much simpler than the rigorous expressions of Eqs. (6.4)–(6.6). Although the IRPA can usually be fitted to low wavevector experimental scattering data, and an "apparent chi-parameter" thereby extracted, the *literal* use of the IRPA for the calculation of thermodynamic properties and phase stability is generally expected to represent a poor approximation due to the importance of density-fluctuation-induced "compressibility" or "equation-of-state" effects [2, 65, 66]. The latter are nonuniversal, and are expected to increase in importance as the structural and/or intermolecular potential asymmetries characteristic of the blend molecules increase.

The conditions required for accuracy of an incompressibility assumption at the level of the scattering functions and spinodal condition are easily derived within the PRISM formalism [67]. From Eq. (6.7) a small isothermal compressibility implies that $-\rho\hat{C}_{MM'}(0) \gg 1$, which is generally true for any dense fluid. If the related wavevector-dependent condition

$$-\rho_M \hat{\omega}_M(k)\hat{C}_{MM}(k) \gg 1 \tag{6.11}$$

applies then considerable simplification of Eqs. (6.4) occurs [67]:

$$\begin{aligned}
\hat{S}_{AA}^{-1}(k) &\cong \frac{\tilde{\Lambda}(k)}{-\rho_A\rho_B\hat{\omega}_A(k)\hat{\omega}_B(k)\hat{C}_{BB}(k)} \\
&\cong (\rho_A\hat{\omega}_A(k))^{-1} + (\rho_B\hat{\omega}_B(k))^{-1}\frac{\hat{C}_{AA}(k)}{\hat{C}_{BB}(k)} \\
&\quad - \hat{C}_{BB}^{-1}(k)\{\hat{C}_{AA}(k)\hat{C}_{BB}(k) - \hat{C}_{AB}^2(k)\} \\
\hat{S}_{BB}^{-1}(k) &\cong \frac{\hat{C}_{BB}(k)}{\hat{C}_{AA}(k)}\hat{S}_{AA}^{-1}(k) \quad \hat{S}_{AB}^{-1}(k) \cong -\frac{\hat{C}_{BB}(k)}{\hat{C}_{AB}(k)}\hat{S}_{AA}^{-1}(k) .
\end{aligned} \tag{6.12}$$

Equation (6.11) can be viewed as an "*effective incompressibility condition*", which is expected to be accurate on long length scales for dense, high polymer blends. However, the interrelationship between the three partial structure factors is not precisely given by the literal incompressibility relations: $\hat{S}_{AA}(k) = \hat{S}_{BB}(k) = -\hat{S}_{AB}(k)$, and the form of $\hat{S}_{AA}(k)$ is not the same as the IRPA-like expression of Eqs. (6.9). Most significantly, the analog of the effective chi-parameter is not of the simple linear arithmetic difference form (see Eqs. (6.16) below), but is fundamentally nonlinear in the direct correlation functions. These differences between the "effective" and "literal" incompressible approximations are generally very important [67]. Similar general conclusions have been drawn by Freed and co-workers [2].

An alternative approach to extracting an apparent chi-parameter from SANS data is to fit the scattering curves to an IRPA form over the entire measured wavevector range. Using Eqs. (6.12) one obtains for the scattering profile in the "effectively incompressible" approximation:

$$\hat{S}_c(k) \equiv \rho^{-1} \sum_{M,M'} b_M b_{M'} \hat{S}_{MM'}(k) = F_A \tilde{S}_c(k) \tag{6.13a}$$

where the "amplitude" factor, F_A, and dimensionless concentration fluctuation scattering function, $\tilde{S}_C(k)$, are given by

$$F_A \equiv b_A^2 \sqrt{\frac{C_{BB}}{C_{AA}}} + b_B^2 \sqrt{\frac{C_{AA}}{C_{BB}}} - 2b_A b_B \frac{C_{AB}}{\sqrt{C_{AA}C_{BB}}} \tag{6.13b}$$

$$\tilde{S}_c^{-1}(k) \equiv \frac{\rho}{\rho_A \hat{\omega}_A(k)} \sqrt{\frac{C_{BB}}{C_{AA}}} + \frac{\rho}{\rho_B \hat{\omega}_B(k)} \sqrt{\frac{C_{AA}}{C_{BB}}} - \rho \frac{C_{AA}C_{BB} - C_{AB}^2}{\sqrt{C_{AA}C_{BB}}} . \tag{6.13c}$$

Here, ρ is the total site number density, and the small angle scattering approximation $\hat{C}_{MM'}(k) \cong \hat{C}_{MM'}(0) \equiv C_{MM'}$ has been employed. The wavevector dependence is contained in $\tilde{S}_C(k)$ which is of the same general mathematical form as the empirical IRPA expression. To make direct contact with the experimental data analysis $\tilde{S}_C(k)$ can be equated to the IRPA form of Eq. (6.9). The result of this procedure is an explicit expression for the apparent SANS chi-parameter. For the simpler case of equal A and B site volumes (generalizations are straightforward) one obtains [67]:

$$\hat{\chi}_s(k) = \frac{\rho}{2\sqrt{C_{AA}C_{BB}}}(C_{AA}C_{BB} - C_{AB}^2) + \frac{1 - \sqrt{C_{BB}/C_{AA}}}{2\phi_A \hat{\omega}_A(k)} + \frac{1 - \sqrt{C_{AA}/C_{BB}}}{2(1-\phi_A)\hat{\omega}_B(k)} . \tag{6.14}$$

Note that the apparent SANS chi-parameter can acquire a k-dependence even in the small angle regime via a "cross-term" between the intramolecular and

intermolecular correlation contributions. Thus, the wavevector dependence may be viewed as an "artifact" of the incompressibility approximation. It may be particularly important for SANS experiments on strongly structurally asymmetric mixtures for which the quantity $|1 - C_{BB}/C_{AA}|$ is expected to be non-negligible. Such an "anomalous" k-dependent chi-parameter has been experimentally observed recently by Brereton et al. [57] in a binary blend of polymers with significantly different aspect ratios (polystyrene and polytetramethyl carbonate). For most amorphous blends composed of relatively flexible chains, experimental SANS data can apparently be adequately fitted using the IRPA and a single, wavevector-independent chi-parameter [56–58]. The latter can be identified with the k = 0 limit of Eq. (6.14):

$$\hat{\chi}_s(k) = \frac{\rho}{2\sqrt{C_{AA}C_{BB}}}(C_{AA}C_{BB} - C_{AB}^2) + \frac{1 - \sqrt{C_{BB}/C_{AA}}}{\phi_A N_A} + \frac{1 - \sqrt{C_{AA}/C_{BB}}}{(1 - \phi_A)N_B} . \tag{6.15}$$

The results of PRISM theory can be substituted in this relation to make contact with SANS experiments which extract an apparent chi-parameter via the k-dependent fitting procedure. Note, however, that in general the predictions of an apparent SANS chi-parameter using Eq. (6.15) will not be the same as the extrapolated zero angle intensity approach of Eq. (6.8). This point re-emphasizes the phenomenological nature of the single, effective chi-parameter approach.

In our initial PRISM studies of polymer blends a literal connection with the IRPA was derived [59, 61] and utilized in model calculations of the effective chi-parameter [59–63]. The incompressibility assumption is fundamentally incompatible with the PRISM approach which naturally includes pure density, pure concentration, and coupled density-concentration fluctuations on all length scales. However, a "literal incompressibility constraint", i.e. $\rho_A(r) + \rho_A(r) = \rho$, can be enforced on the PRISM theory in a post facto manner by employing a functional Taylor expansion of the free energy [59, 61]. This procedure results in a single scattering function of precisely the IRPA form of Eq. (6.9), but the apparent chi-parameter is a wavevector dependent correlation function which we denote here as $\hat{\chi}_{INC}(k)$. In the long wavelength limit, $\hat{\chi}_{INC}(k) \cong \chi_{INC}$ and is given by [61]

$$2\chi_{INC} = \rho[\phi_A r^{-1/2} + \phi_B r^{1/2}]^{-1} \times [r^{-1}\hat{C}_{AA}(0) + r\hat{C}_{BB}(0) - 2\hat{C}_{AB}(0)\} . \tag{6.16}$$

If the blend possesses segmental volume and degree of polymerization symmetries, i.e., r = 1 and $N_A = N_B = N$, then Eqs. (6.16) and (6.10) become particularly simple:

$$2\chi_{INC} = \rho[C_{AA} + C_{BB} - 2C_{AB}] \tag{6.17}$$

$$2\chi_{INC}\phi(1 - \phi)N = 1 \tag{6.18}$$

where Eq. (6.18) applies at the spinodal. Note the analogy here with Flory-Huggins theory. χ_{INC} is a generalization of the incompressible mean field chi-parameter where the k = 0 component of the direct correlation functions replace the "bare" attractive tail potentials. These direct correlation functions contain the many body correlation information neglected by the simple mean field approximation.

Most prior PRISM predictions [23, 59–63] for the effective SANS chi-parameter were based on the literal incompressible form of Eq. (6.16), and not the more experimentally appropriate relation of Eq. (6.8) or (6.15). Thus, it is instructive to inquire whether there are any special cases and/or well-defined additional approximation for which Eqs. (6.6) and (6.12) reduce to the literal IRPA forms. As discussed in Sect. 8 and elsewhere [61, 67, 68], the one special case corresponds to the theoretically much studied, but experimentally unrealizable, "*symmetric polymer blend*". More generally, the additional approximation required to recover the IRPA forms corresponds in integral equation language to the k = 0 statement [67]:

$$C_{MM'} \cong C_0 - \beta v_{MM'}, \quad \text{with} \quad -C_0 \to \infty \ . \tag{6.19}$$

The motivation for this approximation is that the integrated strength of the direct correlation functions (often viewed as "excluded volume parameters") consists of a purely repulsive part plus a weak attractive contribution. If the former is viewed as the bare singular hard core potential (i.e., a literal $\rho \to \infty$ incompressibility approximation for the direct correlation function), then Eq. (6.19) is obtained. Substitution of Eq. (6.19) in Eqs. (6.12) yields the literal IRPA results, with an effective *enthalpic* chi-parameter given by the simple arithmetic difference Flory form of Eq. (6.17) expressed solely in terms of the "weak attractive" contributions $\beta v_{MM'}$. The new molecular closures [68–70] discussed in Sect. 8 do possess a mathematical structure very similar to Eq. (6.19), but with two crucial differences. First, the large repulsive force contributions are not infinite since real liquids are compressible, and second, in general they depend on the two interacting sites (i.e. M and M′ labels) since the local interchain correlations are sensitive to molecular structure. Even in the hypothetical $\rho \to \infty$ limit, the repulsive interaction contribution to $C_{MM'}$ is generally species-dependent which destroys the reduction of Eqs. (6.6) and (6.12) to the literal IRPA forms.

6.3 Other General Aspects

In this paper we focus solely on the spinodal as a measure of the phase behavior. The corresponding binodal can be derived by (numerically) integrating the compressibility relations. Alternatively, the phase behavior could be deduced directly via the so-called "free-energy", or charging parameter route discussed in Sect. 4. Implementation of the "free energy" route is generally much more demanding computationally and has only very recently [70b] been numerically studied within the blend PRISM formalism. Constant volume, not constant

pressure, conditions are assumed. The latter requires a theory for the equation-of-state of blends which has not yet been fully developed. This restriction motivates consideration primarily of upper critical solution temperature (UCST) phase transitions, although some PRISM work on the lower critical solution temperature (LCST) phenomenon has recently been done [67, 71].

Specific results require two additional pieces of information. First, the single chain polymer structure as contained in the species-dependent structure factors must be known. In principle, these correlation functions should be self-consistently computed along with the intermolecular pair correlations. This most rigorous approach is now feasible and is briefly discussed in Sect. 10. However, all published PRISM work on blends has employed the "Flory ideality ansatz" discussed in Sect. 2, i.e., the required $\hat{\omega}_M(k)$ functions are presumed given and effectively independent of blend composition and proximity to the spinodal. To date, published analytical and numerical work for alloys has employed coarse-grained models such as the Gaussian, freely-jointed, and semi-flexible chain. Second, a closure approximation is required which relates the intermolecular pair and direct site-site correlation functions outside the hard core diameter. Both traditional "atomic" and novel "molecular" closures have been studied.

7 Athermal Blends

The model "athermal blend" is defined [59, 62] as the hypothetical limit of vanishing interchain attractive potentials relative to the thermal energy, i.e., $\beta v_{MM'}(r) = 0$. For this situation the atomic site-site Percus-Yevick closure approximation of Eq. (2.7) is employed where the subscripts now refer to the species type. The constant volume athermal blend is of theoretical interest since it isolates the purely entropic packing effects. However, as emphasized by several workers [2, 62, 63, 67], the athermal reference blend is not an adequate model of any real phase separating system. Its primary importance is as a "reference" system for the theories of thermally-induced phase separation discussed in Sect. 8.

A number of numerical PRISM studies [59, 61, 62] of model athermal blends have performed at various levels of single chain description. These mixtures are characterized by structural asymmetries between the two components of either a local nature (size and/or stiffness differences) or global nature (chain length difference, blend of rings and chains). When Gaussian models are employed, numerical studies to date show that these blends are completely miscible in the sense that no spinodal instability is found. However, for dense mixtures of rods and coils [71] and semiflexible chains [72] very recent work has found entropy-driven phase separation. For very stiff polymers, the constant volume assumption, and the neglect by RISM of significant orientational correlations and nematic phase formation [26], may make constant volume PRISM less appropriate.

Typical results [62] for the intermolecular concentration correlations of amorphous Gaussian chain athermal blends are shown in Fig. 9. The amplitude of the structural fluctuations is relatively small. The stiffness/size asymmetric mixture exhibits primarily local deviations from random mixing which decay to zero monotonically with increasing spatial separation. On the other hand, the bimodal chain length blend displays nonmonotonic fluctuations which change sign and peak on a length scale characteristic of macromolecule size. The amplitude of the structural fluctuations in athermal semiflexible polymer mixtures increases significantly as the magnitude of the aspect ratio and/or the difference in persistence lengths of the components increase [71, 72], and phase separation can eventually occur.

The incompressible chi-parameter defined in Eq. (6.16) has also been extensively studied. Many of the numerical results for site volume and/or statistical segment length asymmetric athermal Gaussian chain blends are adequately reproduced at a qualitative level by the analytic thread model discussed in Sect. 2. For an athermal stiffness blend of very long Gaussian threads the k = 0 direct correlation functions are [23, 62]:

$$C_{BB}^{(0)} = \gamma^4 C_{AA}^{(0)} \quad \text{and} \quad C_{AB}^{(0)} = \gamma^2 C_{AA}^{(0)} \tag{7.1}$$

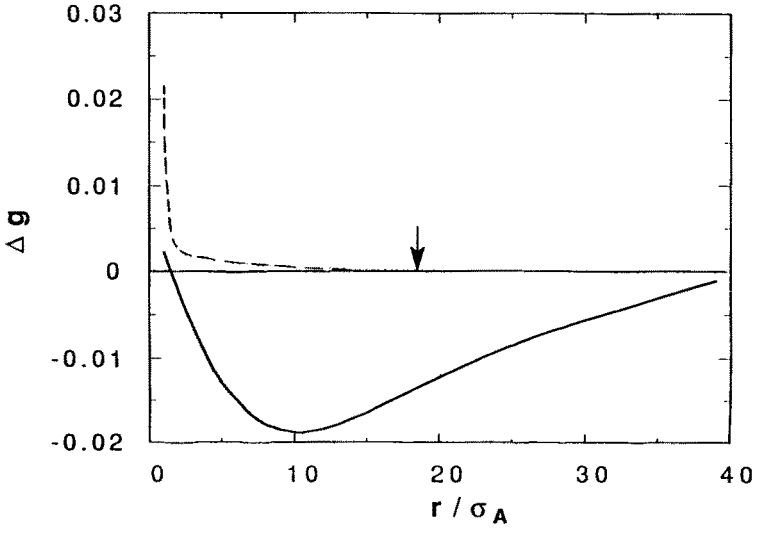

Fig. 9. Intermolecular fluctuation correlation function, $\Delta g(r) = g_{AA}(r) + g_{BB}(r) - 2g_{AB}(r)$, as a function of interchain site separation normalized by the statistical segment length of the A-chain ρ_A(which equals the site hard core diameter). This function is one measure of the length-scale-dependent non-random packing in the mixture. A Gaussian chain model is employed and the volume fraction of A and B chain segments are equal [62]. For completely random mixing $\Delta g(r) = 0$. The *dashed curve* is for a stiffness/size asymmetric case of $\gamma = \sigma_B/\sigma_A = 1.2$ with $N = 2000$ and total packing fraction of 0.45. The *solid curve* is for the bimodal chain length blend with $N_A = 2000$, $N_B = 200$ and a total packing fraction of 0.5. The *arrow* denotes the radius-of-gyration of a 2000 unit ideal Gaussian chain

$$\sigma_A^{-3} C_{AA}^{(0)} = -\frac{\pi^2}{108} \rho \sigma_A^3 [\phi_A + \gamma^2(1 - \phi_A)]$$

$$= -\frac{\pi}{18} \eta \Gamma^3 [\phi_A + \gamma^2(1 - \phi_A)] \tag{7.2}$$

where $\gamma = \sigma_B/\sigma_A$ is the stiffness (or statistical segment length) asymmetry ratio, $\Gamma = \sigma_A/d$ is an aspect ratio, and the superscript "0" emphasizes the results are for athermal blend. Substituting these expressions in Eq. (6.16) yields a negative incompressible chi-parameter:

$$\chi_{INC}^{(0)} = -\frac{\eta^2 \Gamma^6}{6} (\gamma^2 - 1)^2 [\phi_A + \gamma^2(1 - \phi_A)] . \tag{7.3}$$

This result implies that stiffness asymmetry stabilizes the constant volume athermal blend in the sense that pure concentration fluctuations are reduced relative to the $\gamma = 1$ melt. Moreover, within a literal incompressible description it is tempting to conclude from Eq. (7.3) that statistical segment length asymmetry will always decrease the effective chi-parameter and stabilize the miscible phase of real blends. Such a conclusion is generally incorrect with regards to real phase-separating mixtures since it ignores compressibility effects which destroy a rigorous separation of enthalpic and entropic contributions to the thermodynamics of mixing. The irrelevance of a negative chi-parameter for the model athermal blend to the question of miscibility in real polymer mixtures is not a failing of the PRISM theory, but rather only the RPA-like definition of an incompressible chi-parameter in Eq. (6.16). Although perhaps not emphasized enough in early papers, we have explicitly demonstrated that an incompressible idealization, and hence a single chi-parameter, is a poor approximation for a thermal blends [62, 63, 67, 72].

8 Thermally Phase-Separating Blends

A natural foundation for developing an integral equation theory for phase-separating polymer alloys would be an understanding of atomic and small molecule fluid mixtures. Unfortunately, very little work has been done on such systems, and only recently have atomic mixture calculations based on various closure approximations begun to be systematically done and compared with computer simulations [65]. Even less work has been performed for small molecule mixtures using the RISM formalism. From a fundamental theoretical perspective, an accurate treatment of fluctuations induced by the attractive branch of the intermolecular potential is difficult even for simple atomic fluids [5, 6]. These considerations suggest that integral equation theories of polymer alloys should initially focus on the simplest possible mixture in order to test the unavoidable closure approximation.

8.1 Symmetric Blends and Predictions of Atomic Closures

A "symmetric" binary blend is defined as consisting of two types of homopolymer chains, A and B, which are structurally identical in every respect. Hence, the corresponding single chain structure factors obey the identity $\omega_A(r) = \omega_B(r) \equiv \omega(r)$. The pair potentials between sites are:

$$u_{AA}(r) = u_{BB}(r) = u_0(r) + v_{AA}(r)$$

$$u_{AB}(r) = u_0(r) + v_{AB}(r) \tag{8.1}$$

where $u_0(r)$ is a hard core potential with diameter d, and the $v_{MM'}(r)$ potentials are defined for $r > d$. For the "fully symmetric" case of equal concentration of A and B chains there is complete symmetry between A and B, and long wavelength concentration fluctuations are expected to be accurately described by the IRPA-like formula [61, 67]:

$$\hat{S}_c^{-1}(k) = [\hat{\omega}(k)[\phi(1-\phi)]]^{-1} - 2\hat{\chi}_{INC}(k) \tag{8.2}$$

where

$$\hat{\chi}_{INC}(k) = \rho\Delta\hat{C}(k) \equiv \rho[\hat{C}_{AA}(k) - \hat{C}_{AB}(k)] \tag{8.3}$$

and $\phi = 1/2$ for the fully symmetric blend. The "incompressible chi-parameter" is given by the zero wavevector limit of Eq. (8.3), i.e. $\chi_{INC} = \hat{\chi}_{INC}(k = 0)$. The corresponding "mean field" or "bare" chi-parameter, denoted χ_0, is a purely energetic quantity given by:

$$\chi_0 = \beta\rho \int d\vec{r}\{v_{AB}(r) - v_{AA}(r)\} \equiv \beta\rho\{\hat{v}_{AB}(0) - \hat{v}_{AA}(0)\} \tag{8.4}$$

which is the "classical" Flory-Huggins result for the off-lattice situation. Physically, Eq. (8.4) assumes that the intermolecular interactions and chain connectivity induce neither density nor concentration fluctuations in the blends, i.e. a literal random mixing assumption. The quantity χ_{INC}/χ_0 will be referred to as the "renormalization ratio" which serves as a simple scalar measure of the influence of intra- and intermolecular correlations.

Curro and Schweizer have carried out numerical [60, 61] and analytical [23] studies of the symmetric blend using the Mean Spherical Approximation (MSA) closure successfully employed for atomic, colloidal, and small molecule fluids [5, 6]. This closure corresponds to the approximation:

$$C_{MM'}(r) \cong -\beta v_{MM'}(r), \quad r > d\,. \tag{8.5}$$

It is important to emphasize that the PRISM theory with "atomic site-site closures" assumes that all the consequences of chemical bonding are adequately accounted for via the structure of the integral equations alone. As depicted in Fig. 10, even at the two molecule level there are "indirect" pathways by which

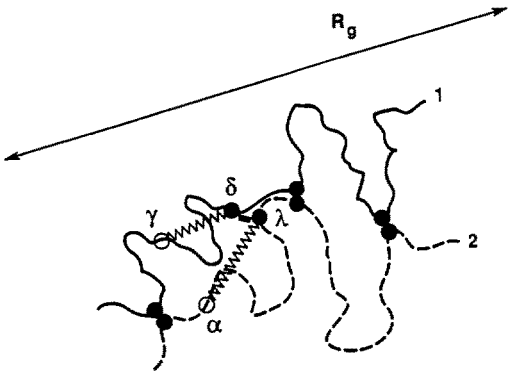

Fig. 10. Schematic representation of two-polymer molecule correlation pathways. The *wiggly bonds* denote long range chemical bonding pair correlations due to chain connectivity, while the *short solid line* denotes the spatially local direct correlation function. There are of order $a + bN^{\theta}$ pair "contacts" between two interpenetrating polymer chains of degree of polymerization N which are embedded in a correlation volume of linear dimension $R_g \propto N^{1/d_F}$. Here d_F is the mass fractal dimension of the polymer, $\theta = 2 - (D/d_F)$, D is the spatial dimension, and a and b are numerical constants of order unity

two particular sites α and γ on different molecules may interact. As a consequence, RISM is never exact even in the "weak coupling" regime where the "tail" potential obeys the inequality $\beta v_{MM'}(r) \ll 1$.

The most provocative prediction of the PRISM-MSA theory was a non-classical relation between the critical temperature for phase separation, T_c, and degree of polymerization, N, of the form $T_c \propto N^{1/2}$. This unexpected result corresponds to a massive stabilization of the mixed phase (via a long range concentration fluctuation process) relative to Flory-Huggins mean field theory which predicts $T_c \propto N$. Moreover, in the high temperature limit, $\chi_{INC}/\chi_0 \propto N^{-1/2}$, thereby implying that the Flory-Huggins form is not recovered even in the perturbative or weak coupling limit of $\chi_0 \to 0$. This fact establishes the important conclusion that the origin of the massive renormalization effect is a two-molecule correlation process which depends on both spatial and polymer fractal dimensionalities [23]. Although there are a number of experiments [58] on more chemically complex alloys which display significant deviations from Flory-Huggins scaling and exhibit N-dependent apparent chi-parameters in the direction predicted by PRISM-MSA, definitive work on simple systems has been lacking.

Very recently, Deutsch and Binder [73] carried out a large scale lattice Monte Carlo simulation on a model symmetric polymer mixture, and Gehlsen et al. [74] performed a SANS study on a family of specially-designed high molecular weight isotopic blends. The classical Flory-Huggins scaling law was found to a high degree of accuracy. This strongly suggests that the PRISM theory with the atomic-like MSA closure is in qualitative error, and our prior PRISM calculations [60, 61, 63] on thermally phase-separating model blends

are not generally reliable. This difficulty motivated Yethiraj and Schweizer to numerically investigate alternative atomic-like site-site closures such as the Percus-Yevick (PY) and Hypernetted Chain (HNC) approximations [70]. From the compressibility route to the thermodynamics nonclassical scaling of T_c with N was again found which disagreed with mean field theory even more strongly than the MSA prediction. Since essentially all liquid state closure approximations are based on the PY, MSA and/or HNC ideas, Yethiraj and Schweizer [68, 70] were forced to the disconcerting conclusion that, based on the compressibility route to the thermodynamics, no known atomic-like closure to the PRISM equations for random coil polymer blends agrees with the classified Flory-Huggins scaling of T_c with N. It appears that quantitative deficiencies associated with atomic site-site closures for the description of attractive interactions in small molecule fluids become grossly amplified into qualitative errors for phase-separating macromolecular systems.

One possible alternative theoretical approach is to calculate the blend thermodynamics and phase diagram not from the compressibility and spinodal divergence, but from the so-called free energy route [5, 6]. As emphasized very recently by Chandler [75], only the spatially local consequences of the attractive potentials on the interchain correlations enter the free energy approach. Thus, long wavelength difficulties of integral equation theories will be "cut off" and a classical $T_c \propto N$ scaling law is obtained [75]. However, there remain severe conceptual difficulties since PRISM-MSA theory is characterized by a massive (N-dependent) thermodynamic inconsistency problem. Moreover, the description of concentration fluctuations on the macromolecular and longer length scales in the one-phase region, which are of prime importance in SANS measurements on blends and microphase separation of diblock copolymers, will still be treated in a qualitatively incorrect fashion at all temperatures [68–70].

8.2 Molecular Closures and Predictions for Symmetric Blends

The theoretical difficulties described in the preceding section have lead Yethiraj and Schweizer to reconsider the question of the closure approximation for interaction-site molecular and polymer fluids [68–70]. Their approach to formulating new "molecular" closures is strongly motivated by the observation that the fundamental error incurred by the atomic-like closures for long wavelength correlations appears in the weak coupling limit [the $\rho \to 0$ two-molecule level for one-component fluids, and the $T \to \infty$ high temperature regime in blends], and is associated with the influence on the site-site direct correlation functions of the number of contacts between a pair of interacting macromolecules. The construction of the new molecular closures is not based on the individual site-site correlation functions, but rather on their full two-molecule counterpart.

Technical development of the new closures has been guided by three general considerations. (1) Separate approximations are employed to treat the consequences of the hard core and (generally attractive) tail parts of the potential.

This strategy is common in atomic fluid theory at low to moderate densities, and for Coulombic systems, and corresponds to the "reference" idea ubiquitous in liquid state theory [5]. The purely hard core problem is treated using the accurate [27] PY closure. (2) The construction of a closure approximation for the tail part of the potential is subject to the constraint of exactly describing the weak coupling limit. In physical terms, for fractal-like interpenetrating molecules these indirect processes may strongly couple the direct correlation functions associated with those pairs of sites which are in simultaneous contact. The number of such two-molecule pair contacts, N_c, scales with N as [23]:

$$N_c \propto 1 + cN^2/R_g^D \propto 1 + c'N^{2-(\frac{D}{d_f})} \tag{8.6}$$

where c and c' are numerical constants of the order of unity, R_g is the radius-of-gyration, and D and d_f are the spatial and mass fractal dimensionalities, respectively. For ideal coils the number of contacts grows as $\sqrt{N}$ and this geometrical factor is the source of the massive "renormalization" predicted by the PRISM-MSA theory. (3) The relation between the intermolecular attractive potentials and the "direct" part of the interchain correlation processes is estimated based on our present understanding of the analogous problem for simple atomic fluids [5, 6].

The simplest molecular closure based on the above ideas is one that builds in the hard core reference behavior and correctly treats the longer ranged attractive potentials in the weak coupling limit. It is called the "Reference Molecular Mean Spherical Approximation" (RMMSA) and is given in real space for a homopolymer blend by [68–70]

$$\omega_M * C_{MM'} * \omega_{M'}(r) \cong \omega_M * C^{(0)}_{MM'} * \omega_{M'}(r) - \omega_M * \beta v_{MM'} * \omega_{M'}(r), \quad r > d_{MM'} . \tag{8.7}$$

The "reference" direct correlation functions associated with the athermal blend are denoted by $C^{(0)}_{MM'}$, and are computed separately using the Percus-Yevick approximation. There are two distinguishing features of this closure. (1) Even outside the hard core, the direct correlation functions between different pairs of sites on two molecules are explicitly coupled. (2) The site-site direct correlations inside the hard core are intimately coupled to their behavior outside the core. These two features are in strong contrast to the atomic closures, and represent the influence of the indirect, chemical-bonding-mediated processes between two molecules.

A more general formulation consistent with the three considerations enumerated above is given for a *homopolymer* blend by [68]:

$$\omega_M * C_{MM'} * \omega_{M'}(r) \cong \omega_M * C^{(0)}_{MM'} * \omega_{M'}(r) + \omega_M * \Delta C_{MM'} * \omega_{M'}(r), \quad r > d_{MM'} . \tag{8.8}$$

where $\Delta C_{MM'}(r)$ is an approximate atomic site-site closure relation for the attractive branch of the potential. For relatively short ranged attractions, the Percus-Yevick closure is quite accurate [5, 6]. This suggests the approximation [68]:

$$\Delta C_{MM'}(r) \cong [1 - \exp(\beta v_{MM'}(r))] g_{MM'}(r), \quad r > d_{MM'} \tag{8.9}$$

which is non-perturbative in the strength of the tail potentials. The combination of Eqs. (8.8) and (8.9) is called the "Reference-Molecular Percus-Yevick (R-MPY)" closure. The qualitative physical content of this approximation is that the "MSA part" of the closure is corrected by the multiplicative factor of the species-dependent radial distribution function in a manner analogous to the calculation of an internal energy or enthalpy. The influence of local fluctuations on the site-site direct correlation functions are then self-consistently determined via solution of the coupled PRISM equations and closure. A useful simplification of the R-MPY closure corresponds to introducing a high temperature approximation (HTA) into Eq. (8.9):

$$\Delta C_{MM'}(r) \cong -\beta v_{MM'}(r) g^{(0)}_{MM'}(r), \quad r > d_{MM'} \tag{8.10}$$

where the superscript "0" refers to the hard core reference blend. This closure approximation is called the R-MPY/HTA and is conceptually of the R-MMSA form but is expected to be more accurate since the influence of reference system correlations on the attractive force component of the direct correlation functions is included.

Extensive studies of the predictions of the new molecular closure to the blend PRISM theory for the symmetric binary blend have been carried out by Yethiraj and Schweizer [68–70]. Here, a few of their major results are summarized, beginning with the numerical studies. The PRISM equations with the molecular closures can be solved using standard Picard iteration methods and the fast Fourier transform [5, 70].

The reduced critical temperature, $T_c^* = k_B T_c/|\varepsilon|$ where ε is the energy parameter of the repulsive Lennard-Jones tail potential between A and B sites, is plotted vs N in Fig. 11 for the R-MMSA and R-MPY closures and two values of total packing fraction [69, 70]. The latter is defined for the tangent semiflexible chain [24] as $\eta = \pi\rho d^3/6$. A linear scaling law is found with a nonuniversal prefactor that decreases with density. As seen in Fig. 11 and Table 1, the R-MPY predicts a significant reduction of the critical temperature relative to both R-MMSA and Flory-Huggins mean field theory which becomes increasingly significant as the polymer density is lowered [70]. This prediction is easily understood as a consequence of the local correlation hole (at lower densities) on the length scale of the tail potential which drives phase separation. Representative results [70] for the composition dependence of the effective incompressible chi-parameter defined in Eq. (6.17) are shown in Fig. 12. The R-MMSA predicts (not shown) virtually no composition dependence, while the R-MPY exhibits [70a] a parabolic-like, concave-upwards behavior the amplitude of which is a strong function of polymer density and stiffness, but weakly dependent on degree of polymerization over the range of $N \leqslant 200$. However, in the large N limit this composition dependence disappears [70b], consistent with thermodynamic perturbation theory arguments [75]. Note that the R-RMSA closure appears to be nearly the integral equation realization of Flory-Huggins theory for the *symmetric* blend, while the R-MPY exhibits a host of fluctuation corrections associated with local correlations in the blend which are in excellent

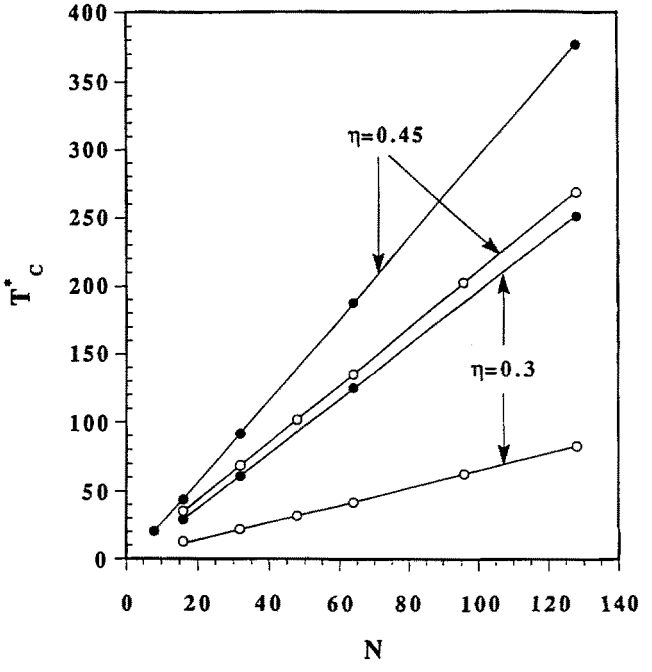

Fig. 11. Variation of the reduced critical temperature, $T_c^* = T_c/\varepsilon$, with degree of polymerization of symmetric binary blends composed of semiflexible chains with zero bending energy [70]. ε is the repulsive AB Lennard-Jones interaction parameter, $v_{AA}(r) = v_{BB}(r) = 0$, and $\phi = 0.5$. Results for the R-MMSA (*solid circles*) and R-MPY (*open circles*) are shown for two values of packing fraction. The *straight lines* are linear fits to the theoretical results for the four highest chain lengths

Table 1. Variation of the ratio of the reduced critical temperature, T_c, predicted by PRISM theory with the R-MPY closure relative to its corresponding mean field Flory-Huggins value, T_0, with packing fraction, η, for a $N = 32$ unit tangent semiflexible chain model [24] (zero bending energy). The interchain tail potentials obey the symmetric restriction with the AA and BB potentials set equal to zero [70]

η	T_c/T_0
0.20	0.126
0.30	0.339
0.45	0.712
0.55	0.930

agreement [70] with recent simulations [73] (with the exception that the critical divergence aspect is not Ising-like).

The density and composition dependent correlation effects present in the R-MPY theory arise from non-random mixing intermolecular packing and

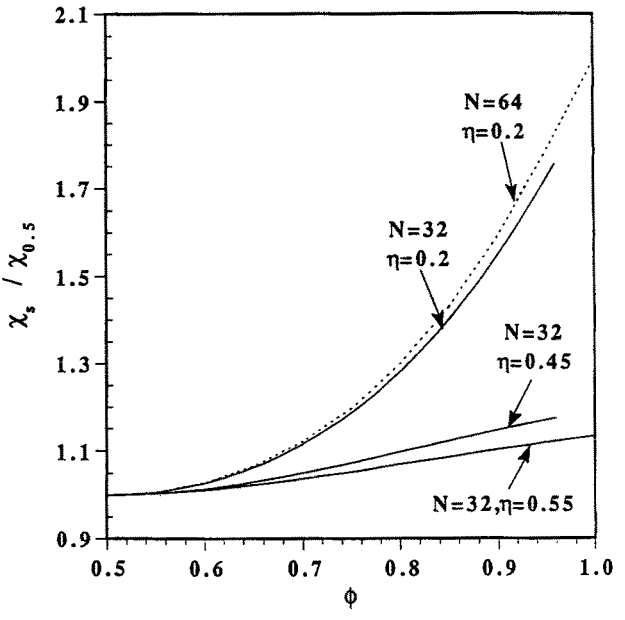

Fig. 12. Numerical predictions of PRISM/R-MPY for the variation with composition of the symmetric blend incompressible chi-parameter (normalized by its values for $\phi = 0.5$) [70]

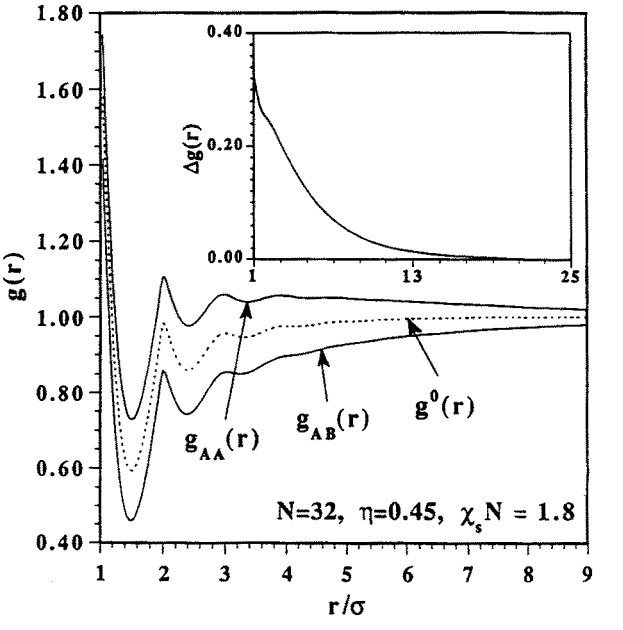

Fig. 13. Intermolecular structure of the $\phi = 0.5$ symmetric blend close to the critical temperature [70]. The *curve labeled* $g^0(r)$ is the corresponding homopolymer melt (infinite temperature) result. The *inset* depicts a measure of the non-random packing expressed as $\Delta g(r) = g_{AA}(r) - g_{AB}(r)$. The behavior of the latter function is qualitatively different when using the atomic MSA closure of the PRISM equations [23, 61, 68]. The radius-of-gyration is 2.91 for N = 32

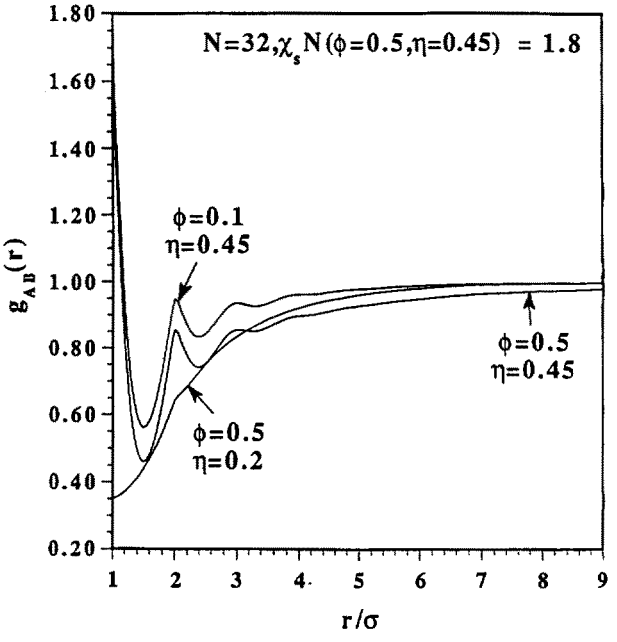

Fig. 14. Selected predictions of PRISM/R-MPY theory for the dependence of the symmetric blend $g_{AB}(r)$ on composition and total packing fraction at fixed temperature [70]

typical results [70] are shown in Figs. 13 and 14. As expected from the discussion of Sect. 8.1, the post facto IRPA simplification is found to be an excellent approximation for the small k scattering functions, effective chi-parameter, and spinodal boundary of the idealized symmetric blend model. The relationship of these calculations for symmetric model blends to experiments on simple isotopic polymer mixtures is discussed elsewhere [67, 68, 70].

Extensive analytic results for the symmetric thread blend have also been derived [68, 70b]. In the thread-polymer limit the hard core condition becomes "irrelevant" for the molecular closure relations. In particular, for the R-MMSA and R-MPY/HTA approximations the $\hat{C}_{MM'}(k)$ functions are fully specified by the closure relations, and their k = 0 values are given in general by

$$\begin{aligned} C_{MM'} &= C^{(0)}_{MM'} - \beta\tilde{H}_{MM'}, \quad d_{MM'} \to 0 \\ \tilde{H}_{MM'} &\equiv v_{MM'}, \qquad\qquad \text{R-MMSA} \\ &\equiv \int d\vec{r}\, v_{MM'}(r) g^{(0)}_{MM'}(r), \quad \text{R-MPY/HTA} . \end{aligned} \tag{8.11}$$

For the symmetric blend the reference system is the homopolymer melt and hence the reference correlation functions are independent of species label (M, M'). It is important to emphasize that Eq. (8.11) is not valid for polymers of nonzero hard core thickness. Thus, the "thread" idealization is a very special limit characterized by a unique simplification of the integral equation theory. These equations have the analytical structure of a "high temperature and/or

mean field" approximation about the hard core blend system at the level of the "effective potentials", i.e., site-site direct correlation functions.

For the symmetric thread blend model, the R-MMSA theory predicts $\chi_{INC} = \chi_0$ for all compositions, densities, etc., and thus represents the integral equation realization of the Flory-Huggins theory with regard to the effective chi-parameter and critical temperature. Such simplicities are a consequence of the "weak coupling" or "asymptotic" nature of a MSA-like closure, i.e., the $r \to \infty$ limit of $g_{MM'}(r) = 1$ is assumed to hold for all r with regards to determining the effects of the attractive potential on the direct correlation functions. MSA and R-MMSA analytical results for the related problems of the liquid-vapor phase transition and polymer-solvent phase separation have also been worked out [68]. Stark differences between the predictions of these two closures of the PRISM equations are again found, with the R-MMSA theory in qualitative agreement with mean field ideas.

The R-MPY/HTA predictions for the symmetric thread blend contain local fluctuation corrections associated with the reference blend correlations. For example, the renormalization ratio in the $N \to \infty$ limit is [68]:

$$\frac{\chi_{INC}}{\chi_0} = \frac{a}{a + \xi_\rho} \tag{8.12}$$

where a is the spatial range of the (screened Coulomb) tail potential and ξ_ρ is the collective density fluctuation length scale of the reference homopolymer melt. The latter length scale decreases monotonically with increasing polymer volume fraction (see, for example, Eq. (3.4a)). Thus the renormalization ratio is predicted to decrease strongly as the polymer density (or spatial range parameter) decreases. However, the renormalization effect vanishes, i.e., $\chi_{INC} = \chi_0$, in the hypothetical $\rho \to \infty$ incompressible limit. The R-MPY/HTA approximation predicts a composition-independent chi-parameter, in disagreement with the full R-MPY numerical results [70] and simulations for the finite N mixtures studied [73]. Thus, the origin of the composition dependence is finite temperature local concentration fluctuations which become monotonically stronger as the spinodal boundary is approached. Perturbation arguments and explicit calculations suggest the HTA should be exact for symmetric mixtures as $N \to \infty$ [5, 70b, 75]. Thus, the "intrinsic" composition-dependence of the effective chi-parameter as computed from the incompressible definition of Eq. (6.17) would vanish for very large N, although compressibility effects could still introduce an apparent composition-dependence in the experimentally relevant SANS chi-parameter as defined in Eqs. (6.8) or (6.15). From a general perspective, the influence of temperature-dependent structural changes on phase behavior is expected to be of considerable importance for polymers of moderate molecular weight, and may be the genesis of the poorly understood lower critical solution temperature (LCST) phenomena commonly observed in polymer blends.

Summarizing, to recover the classic Flory mean field scaling law for the critical temperature within the original compressibility-route PRISM framework requires a reformulation of the closure approximations. The fundamental

quantity susceptible to "simple" approximation appears not to be the site-site direct correlation functions, but its collective two-molecule counterpart, $\omega * C * \omega(r)$. Despite the detailed differences between the R-MMSA, R-MPY and R-MPY/HTA closures, it is important to stress that they are conceptually similar in the sense that globally mean field predictions are obtained in the long chain limit ($T_c \propto N$). The new molecular closures proposed by Yethiraj and Schweizer [68–70] are certainly not unique, and the search for the "most accurate and computationally convenient" closure remains an important problem. The ability to obtain analytical results in the thread limit is a major advantage of the molecular closures described above. We believe the re-formulated PRISM theory of alloys can now be employed to investigate reliably the multitude of physical effects which are beyond mean field and/or lattice approaches.

An alternative approach to circumventing the atomic closure difficulties has very recently been developed by Melenkevitz and Curro [76]. They generalized the "optimized cluster" theory of Chandler and Andersen [77] and Lupkowski and Monson [78] to polymer melts and blends using the diagramatically well-founded RISM formalism [26, 79]. Numerical results for the symmetric blend give the correct mean field scaling of T_C with N, and the effective chi-parameter is found to be weakly composition-dependent.

8.3 Structural and Interaction Asymmetry Effects

"Symmetric polymer blends do not exist in reality. A host of "asymmetries" are present in real chemical alloys of interest. These include attractive potential asymmetries (present even for isotopic blends) and specific interactions, molecular weight asymmetries and polydispersity, and single chain structural differences between the blend components (e.g., monomer shape and volume, backbone stiffness, and tacticity). Realistic accounting for most of these effects would seem to require an off-lattice description which includes local interchain density and concentration correlations, and "compressibility" effects [1, 2, 63, 66, 67, 80].

Detailed analytical and numerical studies of the above questions are in progress, and a very rich and nonadditive dependence of the phase behavior on the precise nature of the attractive potentials, single chain architecture, and thermodynamic state is found [67, 72]. A full understanding of these issues would provide a scientific basis for the rational "molecular design" of polymeric alloys. The influence of asymmetries on the spinodal phase boundary of simple model polymer alloys using analytic PRISM theory with molecular closures has been derived by Schweizer [67]. In this section a few of these results are briefly discussed.

For a binary blend of thread homopolymers the structure of each chain is specified by its statistical segment length, σ_M, segmental hard core diameter, $d_M \equiv d$, degree of polymerization, N_M, and the attractive "tail" potentials, $v_{MM'}(r)$. The structural asymmetry on an equal volume basis is given by the ratio

of statistical segment lengths: $\gamma = \sigma_B/\sigma_A$, which, in general, is temperature dependent. The attractive intermolecular potentials between nonpolar molecules are of the van der Waals or London dispersion form. As a first approximation the corresponding Lennard-Jones energy parameters obey "Berthelot scaling relations":

$$\varepsilon_{BB} = \lambda^2 \varepsilon_{AA}, \quad \varepsilon_{AB} = \lambda \varepsilon_{AA} \tag{8.13}$$

where λ is a positive constant proportional to molecular polarizability and ionization potential ratios [5, 81]. Such scaling relations are also often employed for the integrated strength of the entire attractive potential, $\hat{v}_{MM'}(0)$, or for the internal or cohesive energies in a multicomponent fluid, $\int d\vec{r}\, v_{MM'}(r)\, g_{MM'}(r)$. The latter is the basis of the empirical "solubility" or "Hildebrand" parameter of regular solution theory [82]. These two interpretations correspond to a Berthelot scaling in the analytic thread closures of Eq. (8.11) of the form

$$\tilde{H}_{BB} = \lambda^2 \tilde{H}_{AA}, \quad \tilde{H}_{AB} = \lambda \tilde{H}_{AA}\,. \tag{8.14}$$

The rigorous spinodal boundary is given by Eq. (6.6) and generally strongly differs from that predicted by the literal incompressible RPA approximation of Eqs. (6.10) or (6.18). Analytical results for the spinodal temperature can be derived based on Eqs. (6.6), (7.1), (7.2), (8.11), and (8.14). Other properties such as the critical composition, SANS chi-parameter, free energy of mixing, etc. can also be obtained as discussed in depth elsewhere [67].

For simplicity let $N_A = N_B = N$. The predicted spinodal is [67]:

$$k_B T_S = \frac{\rho |\tilde{H}_{AA}|}{\phi + \gamma^4(1-\phi)} \left\{ N(\lambda - \gamma^2)^2 \phi(1-\phi) + \frac{\phi + \lambda^2(1-\phi)}{-\rho C^{(0)}_{AA}} \right\}. \tag{8.15}$$

Here the "attractive energy scale" variable is

$$|\tilde{H}_{AA}| = |\hat{v}_{AA}(0)|, \quad \text{R-MMSA}$$

$$= |\hat{v}_{AA}(0)| \frac{a}{a + \xi_{EFF}}, \quad \text{R-MPY/HTA} \tag{8.16}$$

where ϕ is the volume fraction of A segments, and ξ_{EFF} is a temperature-independent, but density, composition and aspect ratio dependent, effective density-density screening length in the reference athermal thread blend [67]. The location of the critical composition, and shape of the predicted spinodal envelope, are generally not of classical form due to both stiffness asymmetry and explicit compressibility corrections. For example, the R-MMSA closure predicts the critical composition in the long chain limit is $\phi_c = 1/(1 + \gamma^{-2})$. The dependence of phase separation temperature on statistical segment length asymmetry given by Eq. (8.15) is in excellent agreement [67] with recent experiments by Bates et al. [83] on polyolefin blends and diblock copolymers. The fundamental driving force for phase separation is predicted by compressible PRISM theory

to be enthalpic in nature but with multiple correlation corrections. This aspect is in strong contrast with the recent phenomenological field theory for stiffness asymmetric blends [84] based on a "nematic correlation" process and incompressibility.

The second, "explicit compressibility correction" term in the braces of Eq. (8.15) is essentially N-independent. Since it is positive definite, explicit compressibility effects always destabilize the blend. Its dependence on polymer density is in general very different than the leading "concentration fluctuation" contribution. The latter monotonically increases with polymer density, while the former strongly decreases with density.

The "explicit compressibility contribution" is unimportant if the inequality $-N\rho C_{AA}^{(0)}(\lambda - \gamma^2)^2\phi(1-\phi) \gg 1$ is obeyed. Adopting the latter condition can be viewed as enforcing an "effective incompressibility" constraint in a thermodynamically post facto manner It differs enormously from the spinodal predicted based on the literal IRPA approach of Eqs. (6.17) and (6.18) which is given by [67]

$$k_B T_{S,INC} = \rho|\tilde{H}_{AA}|(\lambda - 1)^2 N\phi(1-\phi)\{1 + (\eta^2\Gamma^6/6)(\gamma^2 - 1)^2 \times N\phi(1-\phi)[\phi + \gamma^2(1-\phi)]\}^{-1} . \quad (8.17)$$

Equation (8.17) incorrectly predicts that increasing stiffness asymmetry monotonically stabilizes the mixture. The basic error incurred by the literal IRPA is the implicit assumption that "enthalpic" and (packing) "entropic" contributions to the non-ideal free energy of mixing are independent and additive.

For the large N and high densities of primary interest in polymer alloy materials, the inequality $-N\rho C_{AA}^{(0)}(\lambda - \gamma^2)^2\phi(1-\phi) \gg 1$ will be violated only for the special case of $\lambda \approx \gamma^2$. However, if such "cancellation" or "compensation" of the attractive potential and stiffness asymmetry factors occurs, then strong stabilization of the blend is predicted since the spinodal temperature obeys the law $T_S \propto N^0$. This suggests an interesting and novel "strategy" for molecular engineering miscible polymer blends or increasing the interfacial region in phase-separated alloys. Equation (8.15) is also consistent with the physical expectation that blends of chains of greatly disparate aspect ratios (e.g., "rods and coils") will phase separate at high temperatures, low N, and/or low total polymer densities, due to packing-induced "frustration". Moreover, if the energetic and structural asymmetries are comparable, then their consequences are never separable since the "cross terms" are always significant and can either stabilize or destabilize the blend depending on the sign of the factor $(\gamma^2 - 1)(1 - \lambda)$. A dramatic example is when $\gamma = 1$, and hence $\chi_0 = 0$, corresponding to an "effectively" athermal case in the mean field sense, but not the literal $\beta v_{MM'}(r) = 0$ athermal situation considered in Sect. 7. Equation (8.15) obviously still predicts phase separation at a temperature which grows strongly with stiffness asymmetry, while the IRPA analysis based on Eqs. (6.17) and (6.18) incorrectly predicts the effective chi-parameter is negative and the blend is completely miscible!

For most of the λ, γ parameter space, correlation effects result in a critical temperature higher than predicted by Flory-Huggins theory [67]. However, there are "windows" of parameter space where stiffness asymmetry stabilizes the blend. Whether the theory predicts relative stabilization or destabilization due to an increase of the stiffness depends crucially on the sign of the quantity $\gamma - \sqrt{\lambda}$.

The apparent SANS chi-parameter is also easily determined analytically for stiffness asymmetric Berthelot thread model with the R-MMSA or R-MPY/HTA closure approximations. For algebraic simplicity we consider the neutron data analysis approach which leads to Eq. (6.15). In the "effectively incompressible" regime, defined here as $|C^{(0)}_{MM'}| \gg |\beta\tilde{H}_{MM'}|$ in Eq. (8.11), one easily obtains the result [67]

$$2\chi_S = \rho\gamma^{-2}\beta|\tilde{H}_{AA}|(\gamma^2 - \lambda)^2 + \frac{1-\gamma^2}{N\phi} + \frac{1-\gamma^2}{N(1-\phi)}. \tag{8.18}$$

This prediction is of the general form found in many SANS experiments, i.e., $\chi_S = A + (B/T)$ where "A" and "B" are often empirically interpretated as "entropic" and "enthalpic" contributions, respectively. Note that for the present idealized thread model, "B" is always positive, but the molecular weight dependent A-factor can in general be positive or negative depending on the precise values of the stiffness asymmetry ratio and blend composition.

In summary, the predictions of analytic PRISM theory [67] for the phase behavior of asymmetric thread polymer blends display a very rich dependence on the single chain structural asymmetry variables, the interchain attractive potential asymmetries, the ratio of attractive and repulsive interaction potential length scales, a/d, and the thermodynamic state variables η and ϕ. Moreover, these dependences are intimately coupled, which mathematically arises within the compressible PRISM theory from "cross terms" between the repulsive (athermal) and attractive potential contributions to the $k = 0$ direct correlations in the spinodal condition of Eq. (6.6). The nonuniversality and nonadditivity of the consequences of molecular structural and interaction potential asymmetries on phase stability can be viewed as a virtue in the sense that a great variety of phase behaviors are possible by rational chemical structure modification. Finally, the relationship between the analytic thread model predictions and numerical PRISM calculations for more realistic nonzero hard core diameter models remains to be fully established, but preliminary results suggest the thread model predictions are qualitatively reliable for thermal demixing [72, 85].

9 Block Copolymers and Other Polymer Alloy Problems

PRISM theory based on the new molecular closures has recently been generalized by David and Schweizer [86] to treat periodic block copolymers. For

simplicity, consider "2M-block copolymers", $(A_xB_y)_M$, which consist of alternating sequences of A and B segments of length x and y, respectively. The following variables are defined: concentration of A-site $f = x/(x + y)$, the total degree of polymerization $N = M(x + y)$, $N_A = xN$, $N_B = yN$, and ρ_{cp} = number density of copolymer molecules. As for the homopolymer case, a tractable theory requires ignoring explicit chain end effects at the level of the direct correlation functions. In addition, an extra zeroth order approximation enters corresponding to neglecting "junction effects". That is, the direct correlation functions associated with a pair of sites of type M and M′ are assumed not to depend on the precise location of the segments within their respective blocks. The resulting matrix PRISM equations in Fourier space are given by [86]:

$$\underline{\hat{H}}(k) = \underline{\hat{\Omega}}(k)\underline{\hat{C}}(k)[\underline{\hat{\Omega}}(k) + \underline{\hat{H}}(k)] \tag{9.1}$$

where the intermolecular site-site pair correlation function matrix is defined as $\hat{H}_{MM'}(k) \equiv \rho_M \rho_{M'} \hat{h}_{MM'}(k)$, $\hat{C}_{MM'}(k)$ is the site-site direct correlation function, and the intramolecular partial structure factor matrix is

$$\hat{\Omega}_{MM'}(k) \equiv \rho_{cp} \sum_{\alpha=1}^{N_M} \sum_{\gamma=1}^{N_{M'}} \hat{\omega}_{\alpha M \gamma M'}(k) \tag{9.2}$$

where $\hat{\omega}_{\alpha M \gamma M'}(r)$ is the normalized probability distribution function where a site α of type M is a distance r from site γ of type M′. It is convenient to introduce a related set of intramolecular correlation functions defined as

$$\hat{\omega}_{MM}(k) \equiv N_M^{-1} \sum_{\alpha,\gamma=1}^{N_M} \hat{\omega}_{\alpha M \gamma M}(k),$$

$$\hat{\omega}_{AB}(k) \equiv (N_A + N_B)^{-1} \sum_{\alpha=1}^{N_A} \sum_{\gamma=1}^{N_B} \hat{\omega}_{\alpha A \gamma B}(k) . \tag{9.3}$$

The collective partial structure factors, $\hat{S}_{MM'}(k)$, are easily written down, and in an approximate theory finite length scale spinodal instabilites *may* be present corresponding to $\hat{S}_{MM'}(k = k^*) = \infty$ which is equivalent to [86]:

$$\begin{aligned} 0 = {} & 1 - f\rho_S \hat{\omega}_{AA}(k^*)\hat{C}_{AA}(k^*) - (1 - f)\rho_S \hat{\omega}_{BB}(k^*)\hat{C}_{BB}(k^*) \\ & - 2\rho_S \hat{\omega}_{AB}(k^*)\hat{C}_{AB}(k^*) + f(1 - f)\rho_S^2 \delta\hat{\omega}(k^*)\delta\hat{C}(k^*) \end{aligned} \tag{9.4}$$

$$\delta\hat{\omega}(k) \equiv \hat{\omega}_{AA}(k)\hat{\omega}_{BB}(k) - f^{-1}(1 - f)^{-1}\hat{\omega}_{AB}^2(k),$$

$$\delta\hat{C}(k) \equiv \hat{C}_{AA}(k)\hat{C}_{BB}(k) - \hat{C}_{AB}^2(k)$$

where k^* is the most unstable wavevector and $\rho_S = N\rho_{cp}$. Since microphase separation is a finite length scale ordering phenomena akin to crystallization, a critical point is not generally expected to exist in physical reality.

The mean field (Landau) theory of block copolymers developed by Leibler [87] is based on an IRPA treatment of the liquid correlations. Enforcing the latter constraint on PRISM theory in a post facto manner yields for an AB block

copolymer for which the A and B site volumes are equal [86]

$$\hat{S}^{-1}_{RPA}(k) = \frac{f\hat{\omega}_{AA}(k) + (1-f)\hat{\omega}_{BB}(k) + 2\hat{\omega}_{AB}(k)}{f(1-f)\hat{\omega}_{AA}(k)\hat{\omega}_{BB}(k) - \hat{\omega}^2_{AB}(k)} - 2\hat{\chi}_{INC}(k) \,. \tag{9.5}$$

The effective chi-parameter is given by the k-dependent generalization of Eq. (6.17). If a small angle approximation where $\hat{\chi}_{INC}(k)$ is constant is invoked, then Eq. (9.5) is identical in form with Leibler's RPA result [87] and the spinodal condition is far simpler than Eq. (9.4). However, since the true "chi-parameter" is a wavevector-dependent correlation function, not a phenomenological number, it is functionally related to all the other intramolecular and intermolecular pair correlations in the system. This non-mean-field feature has many important consequences such as the fact that k* is influenced by many chain correlations [86, 88]. It must be emphasized that although Eq. (9.5) should be accurate for the hypothetical symmetric block copolymer model, since it does not properly treat compressibility effects it is expected to be inadequate for most real copolymer systems.

The same molecular closures proposed for homopolymer blends [68–70] apply to copolymers but the intramolecular structure factor matrix is now non-diagonal. Equation (8.8) becomes [86]

$$[\underline{\Omega} * \underline{C} * \underline{\Omega}(r)]_{MM'} \cong [\underline{\Omega} * \underline{\underline{C^{(0)}}} * \underline{\Omega}(r)]_{MM'} + [\underline{\Omega} * \underline{\Delta C} * \underline{\Omega}(r)]_{MM'}, \quad r > d_{MM'} \,. \tag{9.6}$$

For the analytically tractable thread polymer model, and the R-MMSA or R-MPY/HTA closure approximations, $k = 0$ values of the direct correlation functions are precisely the same in the long chain limit as found for polymer blends in Sect. 8. In particular, for the symmetric block copolymer, the R-MMSA closure yields [67, 86] the mean field result $\chi_{INC} = \chi_0$. Thus, within the symmetric thread idealization and the incompressible approximation of Eq. (9.5), PRISM/R-MMSA theory reduces to Leibler theory for all compositions and block architectures [67, 86].

For the more interesting thread model case with statistical segment asymmetry and a Berthelot attractive potential model, Schweizer has derived the following expression for the spinodal temperature [67]

$$\frac{k_B T_S}{\rho_S |\tilde{H}_{AA}|} = f(1-f)N(\gamma^2 - \lambda)^2 \tilde{F}(k^*, f, \gamma) + [-\rho_S C^{(0)}_{AA}]^{-1} \tilde{G}(k^*, f, \gamma, \lambda) \tag{9.7}$$

where the block architecture-dependent (x and y variables) functions F and G are given by

$$\tilde{F} \equiv N^{-1} \frac{\hat{\omega}_{AA}(k^*)\hat{\omega}_{BB}(k^*) - [f(1-f)]^{-1}\hat{\omega}^2_{AB}(k^*)}{f\hat{\omega}_{AA}(k^*) + \gamma^4(1-f)\hat{\omega}_{BB}(k^*) + 2\gamma^2\hat{\omega}_{AB}(k^*)}$$

$$\tilde{G} \equiv \frac{f\hat{\omega}_{AA}(k^*) + \lambda^2(1-f)\hat{\omega}_{BB}(k^*) + 2\lambda\hat{\omega}_{AB}(k^*)}{f\hat{\omega}_{AA}(k^*) + \gamma^4(1-f)\hat{\omega}_{BB}(k^*) + 2\gamma^2\hat{\omega}_{AB}(k^*)} \,. \tag{9.8}$$

The functions F and G are both independent of N in the long chain limit. For a stiffness symmetric f = 1/2 diblock copolymer in the $N \gg 1$ limit, the quantity F = 2/10.495. The ordering wavevector, k*, is (numerically) determined by maximizing the right hand side of Eq. (9.7), and is a function of all the variables in the problem. Note that the mathematical structure of Eq. (9.7) is qualitatively similiar to the blend case of Eq. (8.15).

As discussed in Sect. 8.3 and elsewhere [67, 68, 86], for the R-MMSA and R-MPY/HTA closures, taking the thread limit results in a theory where the hard core exclusion condition is not relevant (except for determining the reference fluid $C^{(0)}_{MM'}$). This great simplification does not occur for any non-zero hard core diameter. Calculations by David and Schweizer [86] for symmetric diblocks have shown that PRISM with the R-MMSA closure for non-thread symmetric diblocks does not exhibit a critical point or spinodal instabilities if either the temperature or inverse degree of polymerization are nonzero. The destruction of the critical point appears to be a "finite size" fluctuation effect, as in the Brazovski-Fredrickson-Helfand phenomenological field theory [89], but the physical origin of the nonlinear feedback mechanism is very different.

An example of the intermolecular concentration correlations and scattering intensity for a symmetric diblock melt [86] composed of ideal freely-jointed chains are shown in Fig. 15. Note that as the melt is cooled, strong local and

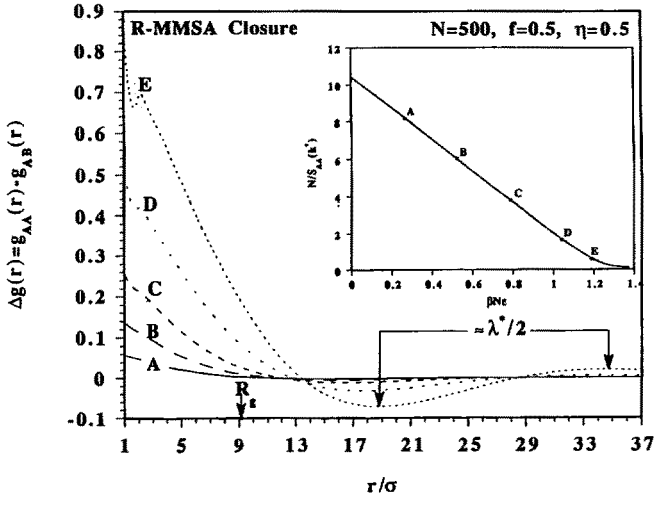

Fig. 15. Temperature dependence of $\Delta g(r) = g_{AA}(r) - g_{AB}(r)$ for the f = 0.5 symmetric diblock copolymer using the R-MMSA closure [86]. An ideal freely-jointed single chain model is employed and the choice of tail potentials is identical to the symmetric blend discussed in Sects. 6 and 8. Note that upon cooling strong local correlations emerge. Eventually a weaker, long range oscillatory feature appears associated with correlations on the domain size length scale ($\lambda^* \cong 2\pi/k^*$). The inset shows the corresponding points (A–E) in the inverse scattering peak intensity $N/S^{(k)}_{AA}$ as a function of dimensionless, scaled inverse temperature $\beta N\varepsilon$. Note the linear "mean field" behavior at high temperatures but the nonlinear stabilization at the low temperatures where the long range oscillation in $\Delta g(r)$ emerges

long wavelength correlations emerge, the detailed nature of which depend on copolymer composition, N, single chain structure, density, etc. Such local fluctuations may be very important for understanding thermodynamic properties and experimental measurements of short and intermediate length scale structure in the diblock melt (e.g., NMR, dielectric spectroscopy, wide angle scattering).

There remains the controversial question of whether "fluctuation phenomena" in diblock copolymers are a finite size effect [89], or an intrinsic process which survives in the $N \to \infty$ limit as recently suggested based on both simulations [88] and non-perturbative theoretical arguments [90]. Numerical PRISM calculations based on the most sophisticated R-MPY closure favor an approximately intrinsic process for symmetric diblocks of $N \leqslant 500$; however, the true asymptotic behavior appears to be a finite size effect [86].

Several other polymer alloy problems have just begun to the investigated using the PRISM approach. These include (a) LCST phase behavior in binary blends where "specific interactions" are present [67, 71]; (b) segregation of blends near a surface and in confined spaces [91a] using the wall-PRISM theory of Yethiraj and Hall [37]; (c) mixtures of statistically random copolymers [67]; and (d) polymer-colloid mixtures [91b]. The application of existing PRISM theory to treat more complex mixtures such as a binary blend plus solvent, or a block copolymer/homopolymer mixture, are straightforward. All these problems will be even richer and more complex with regards to their sensitivity to system-specific structural and interaction potential asymmetries.

10 Self-Consistent PRISM Theory

All the theory described so far has assumed the intramolecular pair correlations are known, and in practice a Flory ideality ansatz is employed. However, even in dense melts and concentrated solutions where the chains are random walks on large length scales, the effective local persistence length may be sensitive to chemical structure and thermodynamic state. For semi-dilute solutions the excluded volume screening length strongly increases and large deviations from ideality occur [3a, 22]. For branched polymers ideality will not be preserved near the branch point(s) even in the melt state. In blends and copolymers concentration fluctuations may be an extra source of conformational perturbations and are poorly understood. The generalization of the PRISM approach to self-consistently calculate intramolecular and intermolecular pair correlations functions has been initiated [92] but is still in its early stages. Here, we sketch the basic ideas, briefly describe one application, and discuss ongoing research.

For simplicity, consider a solution of homopolymers where the "solvent" is treated as "free volume" and thus an effectively one-component description

applies. The single polymer effective potential energy in the condensed phase, W(R), contains three distinct terms [14, 92]

$$W(\underset{\sim}{R}) = U_0 + U_E + \Delta\mu \tag{10.1}$$

where $\underset{\sim}{R}$ denotes a complete set of coordinates which specifies a particular polymer configuration. The "ideal" contribution, U_0, contains all the short range interactions such as bond length and angle constraints, torsional potentials, etc. The "long range" intramolecular potential, U_E, is taken to be pairwise decomposable, and in specific applications to date has been chosen to be a hard core or soft repulsion. The "medium-induced" contribution, $\Delta\mu$, is the excess chemical potential for the polymer constrained to a particular conformation $\underset{\sim}{R}$ due to its interactions with the surrounding molecules. This object is extremely complex since it involves many body correlations.

Chandler and co-workers constructed a tractable medium-induced potential in the context of the solvated electron problem [93, 94]. Their "self-consistent pair" approximation also applies to real polymeric fluids, and for homopolymers with neglect of explicit chain end effects approximation one has [92–94]

$$\Delta\mu \cong \sum_{\alpha,\gamma} w(|\vec{r}_\alpha - \vec{r}_\gamma|), \quad w(r) = -\beta^{-1} C * \rho S * C(r) . \tag{10.2}$$

This result can be deduced from a number of perspectives such as renormalized perturbation theory [93], polymer density functional theory [95, 96], and Percus functional expansion methods [97]. The medium-induced pair potential is determined by the direct correlation function and collective density fluctuations which are both functionally related to the intramolecular pair correlations via the PRISM equation. Hence, a coupled intramolecular/intermolecular theory is obtained.

Implementation of this "self-consistent" PRISM theory is non-trivial and there are two general classes of approach. First, approximate theories can be constructed based on a tractable reference system description of single chain correlations and an approximate free energy. The initial work along this line by Schweizer, Honnell and Curro [92] used an optimized perturbation scheme for dense melts which predicted chain dimensions and intermolecular pair correlations in very good agreement with molecular dynamics simulations [27]. However, this approach is rather limited in the choice of reference system, and does not correctly describe stiff polymers nor long chain semi-dilute solutions [30]. More general variational approaches have been recently developed by several workers [97, 98] which remove these limitations. They have been extensively applied to predict (both analytically and numerically) chain dimensions as a function of polymer concentration, molecular weight, aspect ratio, and global architecture. The best approximation probably depends on the particular system and thermodynamic conditions of interest, and theory development remains an active area of present research.

The second approach is to use Monte Carlo simulation to solve exactly the nonlocal single chain problem (defined by Eqs. (10.1) and (10.2)) self-consistently with the PRISM theory of many chain correlations. Although more computationally demanding, the introduction of an approximate free energy expression and reference system are avoided. The first implementation of this "PRISM/Monte Carlo" (PMC) scheme has been performed by Melenkevitz et al. [96] for the case of homopolymer solutions composed of semiflexible chains [24] (with zero local bending energy). A more extensive PMC study of the same model over the entire range of density from dilute solution to the dense melt using a more sophisticated Monte Carlo algorithm has also been performed [99]. The latter results are summarized in Table 2. The PMC theory with the solvent-induced potential of Eq. (10.2) accurately predicts both the magnitude and density dependence of chain dimensions in semi-dilute and weakly concentrated solutions [96, 99]. However, for concentrated solutions and melts the chains tend to "collapse" locally (not in the $\langle R^2 \rangle \propto N^{2/3}$ global sense), and the physically expected ideal random coil behavior is not recovered [96, 99]. This subtle high density problem is still under active study, but the work of Grayce and co-workers [97, 99] suggests the difficulty lies with the approximate medium-induced potential of Eq. (10.2) which predicts too strong a compressive force at high densities. Both a new solvent-induced pair potential, and a criterion for a priori accessing the accuracy of approximate solvation potentials, have been formulated [97]. Preliminary results are encouraging since PMC with the new solvation potential correctly predicts the qualitative conformational behavior of flexible polymers over the entire density range [99].

Table 2. Mean-square end-to-end distance, $\langle R^2 \rangle$, in units of the hard core diameter, as a function of packing fraction and N. $\langle R^2 \rangle_{PMC}$ refers to the results of [99] using self-consistent PRISM/Monte Carlo based on Eq. (10.2) for a hard core tangent semiflexible chain model [24]. $\langle R^2 \rangle_{MC}$ are the results of many chain "exact" Monte Carlo simulations of Yethiraj and Hall [29]. The corresponding density-independent self-avoiding walk (ideal walk) values of $\langle R^2 \rangle$ are: 50.78 (30.79), 152.03 (80.8), and 348.51 (164.12) for N = 20, 50, and 100, respectively

N	η	$\langle R^2 \rangle_{PMC}$	$\langle R^2 \rangle_{MC}$
20	0.10	45.24 ± 0.41	43.01 ± 1.79
20	0.20	41.92 ± 0.09	37.37 ± 1.32
20	0.30	38.43 ± 0.48	34.95 ± 2.81
20	0.35	35.69 ± 0.49	32.23 ± 4.30
20	0.40	32.39 ± 0.35	
20	0.45	26.56 ± 0.30	
20	0.50	17.76 ± 0.64	
50	0.20	131.57 ± 1.90	118.70 ± 4.83
50	0.30	119.40 ± 1.19	106.84 ± 6.05
100	0.20	299.57 ± 2.55	242.51 ± 6.53
100	0.30	276.67 ± 5.54	220.09 ± 5.08
100	0.40	224.03 ± 5.67	
100	0.45	149.83 ± 15.4	

Formally, the self-consistent PRISM theory is easily generalized to treat polymer blends and copolymers [92] where significant non-ideal conformational effects may occur which intensify as phase separation is approached.

11 Future Directions

The full development and application of many aspects of the PRISM theory discussed in this paper remain to be done. In both melts and alloys, the construction of a "thermodynamically self-consistent" theory is an important task in order to compute accurately the equation-of-state and thereby allow constant pressure calculations to be carried out. This direction may also be important for understanding at a molecular-level LCST phase transitions. Construction of the binodal curve is also an important technical direction, as are careful studies of the free energy-based route to the phase diagram [70b]. Further fundamental research concerning the closure difficulties encountered in phase-separating polymer alloys is an ongoing topic, as is continual testing of the accuracy of PRISM theory against carefully designed off-lattice computer simulations and experimental measurements on model systems.

From the point of view of atomistic modeling, the application of PRISM theory with chemically realistic single chain models, such as the RIS description, is a major thrust of present and planned research particularly in the area of multiphase alloys. The influence of microstructural features such as chain branching (e.g., olefins) [108], monomer shape, and tacticity [71] on packing and phase stability can thus be unambiguously investigated. A priori, one might expect that thermodynamic properties and phase diagrams are extremely sensitive to local chemical structure and packing. However, many theoretical approaches and/or models rely on the hope that for flexible macromolecules a significant amount of "self-averaging" of the Angstrom-level chemical details occurs, and thus intermediate-level models of chain structure are useful. Systematic PRISM studies of polymer models of increasing chemical complexity will allow this subtle and very important question to be addressed.

The combination of polymeric density functional methods and PRISM theory for the liquid correlations allow a wide range of closure and inhomogeneous material problems to be studied [109]. Present research involves using this approach to treat at an atomistic level the crystallization of the entire alkane series, and the structure of hydrocarbon fluids near surfaces and interfaces [109]. An alternative, purely integral equation approach to the latter problem is to employ the wall-PRISM theory of Yethiraj and Hall [37].

The further development of the self-consistent version of PRISM theory will be particularly important in two areas: (i) liquids of flexible conjugated polymers where the electron delocalization length and interchain dispersion forces are strongly coupled to chain conformation [100], and (ii) polymer alloys where

nonuniversal conformational perturbations due to both density and concentration fluctuations are intimately coupled and may significantly influence the location, and perhaps the nature, of the phase boundaries.

The PRISM theory has recently been generalized and applied by Grayce and Schweizer [101] to treat star-branched polymer solutions and melts. For such systems the equivalent site approximation must be abandoned, and non-ideal conformational effects become particularly important near the crowded central branch point. Generalization of their new methods to treat complex fluids composed polymer-coated colloidal particles is also feasible and presently under study.

Other important unsolved general problems within the PRISM formalism include the following. (a) The treatment of quenched randomness, e.g., sequence disorder in random copolymers. (b) The description of first order microphase separation transitions in block copolymers. Polymeric density functional methods, such as recently employed by Melenkevitz and Muthukumar [102], present an attractive strategy. (c) Macromolecular liquids with strong and/or directional attractive forces, such as ionomers and polyelectrolytes. Nonideal conformational perturbations are likely to be particularly important in these systems, and the appropriate closure approximation for Coulombic interactions in macromolecular fluids remains an open question. (d) Polymer liquid crystals, and molecular "composites" composed of rod-like and flexible species. The proper description of strong orientational correlations and/or the nematic phase represent major challenges for site-site integral equation approaches. All the equilibrium structural information calculable from PRISM theory will also find additional applications in microscopic theories of macromolecular dynamics such as the polymeric mode-coupling approach [103].

Finally, we mention that very recently three other integral equation approaches to treating polymer systems have been proposed. Chiew [104] has used the "particle-particle" perspective to develop theories of the intermolecular structure and thermodynamics of short chain fluids and mixtures. Lipson [105] has employed the Born-Green-Yvon (BGY) integral equation approach with the Kirkwood superposition approximation to treat compressible fluids and blends. Initial work with the BGY-based theory has considered lattice models and only thermodynamics, but in principle this approach can be applied to compute structural properties and treat continuum fluid models. Most recently, Gan and Eu employed a Kirkwood hierarchy approximation to construct a self-consistent integral equation theory of intramolecular and intermolecular correlations [106]. There are many differences between these integral equation approaches and PRISM theory which will be discussed in a future review [107].

Acknowledgement. The work described in this paper was done with many excellent collaborators. We gratefully acknowledge the important theoretical contributions of K.G. Honnell, J.D. McCoy, J. Melenkevitz, A. Yethiraj, C.J. Grayce, and E.F. David. We would also like to thank G.S. Grest, K. Kremer and J.D. Honeycutt for fruitful theory/computer simulation collaborations, and A.H. Narten and A. Habenshuss for theory/experiment collaborations. Helpful discussions and/or correspondence with many scientists are also appreciated with a special thanks extended to D. Chandler. We are grateful to C.J. Grayce, G. Szamel, A. Yethiraj, and E.F. David for their critical reading of

this manuscript. The work described in this paper has been done over a period of several years. At Sandia National Laboratories support came from the U.S. Department of Energy under contract DE-AC047DP00789, and also the Basic Energy Sciences/Division of Materials Science Program. Support at the University of Illinois is from the Division of Materials Sciences, Office of Basic Energy Sciences, U.S. Department of Energy in cooperation with the UIUC Frederick Seitz Materials Research Laboratory (via grant number DEFG02-91ER45439) and Oak Ridge National Laboratory. Support from the central computing facilities of the UIUC-MRL are also gratefully acknowledged.

References

1. Flory PJ (1953) Principles of polymer chemistry. Cornell University Press, Ithaca
2. Dudowicz J, Freed MS, Freed KF (1991) Macromolecules 24: 5096; Freed KF, Dudowicz J (1992) Theoretica, Chimica Acta 82; Dudowicz J, Freed KF (1993) Macromolecules, 26: 213; Freed K, Dudowicz J (1992) J Chem Phys 97: 2105
3. (a) For polymer solutions: Doi M, Edwards SF (1986) Theory of polymer dynamics. Oxford Press, Oxford; (b) For block copolymers: Bates FS, Fredrickson GH (1990) Ann Rev Phys Chem 41: 525
4. Roe RJ (ed) (1991) Computer simulations of polymers. Prentice Hall, Englewood Cliffs, N.J.; Colburn EA (ed) (1992) Computer simulations of polymers. Longman, Harlow; Binder K (1993) Advances in Polymer Science, in press
5 Hansen JP, McDonald IR (1986) Theory of simple liquids, 2nd edn. Academic, London
6. Chandler D (1982) In: Montroll EW, Lebowitz L (eds) Studies in statistical mechanics, vol. VIII. North-Holland, Amsterdam, p. 274 and references cited therein
7. Percus JK (1964) In: Frisch HL, Lebowitz KL (eds) Classical fluids. Wiley, New York
8. Chandler D, Andersen HC (1972) J Chem Phys 57: 1930
9. Lowden LJ, Chandler D (1974) J Chem Phys 61: 5228; (1973) 59: 6587; (1975) 62: 4246
10. Chandler D, Hsu CS, Streett WB (1977) J Chem Phys 66: 5231; Sandler SI, Narten AH (1976) Mol Phys 32: 1543; Narten AH (1977) J Chem Phys 67: 2102; Hsu CS, Chandler D (1978) Mol Phys 36: 215 ; Mol Phys 37: 299 (1979)
11. Schweizer KS, Curro JG (1987) Phys Rev Lett 58: 246
12. Curro JG, Schweizer KS (1987) Macromolecules 20: 1928
13. Curro JG, Schweizer KS (1987) J Chem Phys 87: 1842
14. Schweizer KS, Curro JG (1988) Macromolecules 21: 3070
15. Schweizer KS, Curro JG (1988) Macromolecules 21: 3082
16. Volkenstein MV (1963) Configurational statistics of polymer chains. Interscience, New York; Flory PJ (1969) Statistical mechanics of chain molecules. Interscience, New York
17. Flory PJ (1949) J Chem Phys 17: 203
18. Curro JG (1976) J Chem Phys 64: 2496; (1979) Macromolecules 12: 463; Vacatello M, Avitabile G, Corradini P, Tuzi A (1980) J Chem Phys 73: 543
19. Ballard DG, Schelton J, Wignall GD (1973) Eur. Polymer Journal, 9: 965; Cotton JP, Decker D, Benoit H, Farnoux B, Higgins J, Jannick G, Ober R, Picot C, des Cloizeaux J (1974) Macromolecules 7: 863
20. Lue L, Blanckschtein D (1992) J Phys Chem 96: 8582
21. Elliot JR, Kanetar US (1990) Mol Phys 71: 871 and 883
22. deGennes PG (1979) Scaling concepts in polymer physics. Cornell University Press, Ithaca
23. Schweizer KS, Curro JG (1990) Chemical Physics, 149: 105; Schweizer KS, Curro JG (1991) J Chem Phys 94: 3986
24. Honnell KG, Curro JG, Schweizer KS (1990) Macromolecules, 23: 3496
25. Koyama R (1973) J Phys Soc Japan, 22: 1029; Mansfield ML (1986) Macromolecules, 19: 854
26. Chandler D, Silbey RS, Ladanyi BM (1982) Mol Phys 46: 1335; Richardson DM, Chandler D (1984) J Chem Phys 80: 4484
27. Curro JG, Schweizer KS, Grest GS, Kremer K (1989) J Chem Phys 91: 1357; Kremer K, Grest GS (1990) J Chem Phys 92: 5057
28. Andersen HC, Weeks JD, Chandler D (1971) Phys Rev A 4: 1597; Weeks JD, Chandler D, Andersen HC (1971) J Chem Phys 54: 5237

29. Yethiraj A, Hall CK (1991) J Chem Phys 93: 4453; (1992) 96: 797
30. Yethiraj A, Schweizer KS (1992) J Chem Phys 97: 1455
31. McCoy JD, Honnell KG, Curro JG, Schweizer KS, Honeycutt JD, Macromolecules (1992) 25: 4905
32. Honnell KG, McCoy JD, Curro JG, Schweizer KS, Narten AH, Habenschuss A (1991) J Chem Phys 94: 4659
33. Narten AH, Habenschuss A, Honnell KG, McCoy JD, Curro JG, Schweizer KS (1992) J Chem Soc Faraday Trans 88: 1791
34. Honnell KG, McCoy JD, Curro JG, Schweizer KS, Narten AH, Habenshuss A (1991) Bull Am Phys Soc 36(3): 481, and paper in preparation
35. Barker JA, Henderson D (1967) Chem Phys 47: 4714; (1972); Ann Rev Phys Chem 23: 439; (1976) Rev. Mod Phys 48: 587
36. Dickman R, Hall CK (1988) J Chem Phys 89: 3168
37. Yethiraj A, Hall CK (1991) J Chem Phys 95: 3749
38. Yethiraj A, Curro JG, Schweizer KS, McCoy JD (1993) J Chem Phys 98: 1635
39. Curro JG, Yethiraj A, Schweizer KS, McCoy JD, Honnell KG (1993) Macromolecules 26: 2655
40. Dickman R, Hall CK (1986) J Chem Phys 85: 4108; Honnell KG, Hall CK (1989) J Chem Phys 90: 1841
41. Olabisi O, Simha R (1975) Macromolecules 8: 206
42. Lopez-Rodriguez A, Vega C, Freire JJ, Lago S (1991) Mol Phys 73: 691
43. Martynov GA, Vompe AG (1993) Phys Rev E 47: 1012
44. Flory PJ (1956) Proc Roy Soc A 234: 60
45. Nagle JF, Gujrati PD, Goldstein M (1984) J Phys Chem 88: 4599
46. Ramakrishnan TV, Yussouff M (1979) Phys Rev B 19: 2775
47. Haymet ADJ, Oxtoby DW (1981) J Chem Phys 74: 2559; Laird BB, McCoy JD, Haymet ADJ (1987) J Chem Phys 87: 5451
48. Chandler D, McCoy JD, Singer SJ (1986) J Chem Phys 85: 5977; McCoy JD, Singer SJ, Chandler D (1987) J Chem Phys 87: 4953
49. McCoy JD, Rick SW, Haymet ADJ (1989) J Chem Phys 90: 4622; (1990) 92: 3034; Rick SW, McCoy JD, Haymet ADJ (1990) J Chem Phys 92: 3040
50. Ding K, Chandler D, Smithline SJ, Haymet ADJ (1987) Phys Rev Lett 59: 1698
51. McMullen WE, Freed KF (1990) J Chem Phys 92: 1413
52. McCoy JD, Honnell KG, Schweizer KS, Curro JG (1991) Chem Phys Lett 179: 374; J Chem Phys 95: 9348
53. Wunderlich B, Czornj G (1977) Macromolecules 10, 906
54. Starkweather HW, Zoller P, Jones GA, Vega AJ (1982) J Polym Sci., Polym Phys 20: 751
55. See, for example, Bates FS (1991) Science 251: 898; Sanchez IC (1983) Ann Rev Mater Sci 13: 387; Solc K (ed) (1981) Polymer compatibility and incompatibility. Midland, Michigan
56. Wignall GD (1987) in Encyclopedia of polymer science and engineering, second edition. Wiley, New York, vol. 12, p. 112
57. See, for e.g., Jung WG, Fischer EW (1988) Makromol, Chem Makromol Symp 16: 281; Brereton MG, Fischer EW, Herkt-Maetzky C, Mortensen K (1987) J Chem Phys 87: 6114; Han CC, Bauer BJ, Clark JC, Moroga Y, Matsushita Y, Okada M, Tran-cong Q, Chang T, Sanchez IC (1988) Polymer 29: 2002; Bates FS, Muthukumar M, Wignall GD, Fetters LJ (1988) J Chem Phys 89: 535
58. Marie P, Selb J, Rameau A, Gallot Y (1988) Makromol Chem Makromol Symp 16: 301; Jung WG, Fischer EW (1988) ibid 16: 281; Hashimoto T, Ijichi Y, Fetters LJ (1988) J Chem Phys 89: 2463; Ijichi Y, Hashimoto T, Fetters LJ (1989) Macromolecules 22: 2817; Tanaka H, Hashimoto T (1991) Macromolecules 24: 5398
59. Schweizer KS, Curro JG (1988) Phys Rev Lett 60: 809
60. Curro JG, Schweizer KS (1988) J Chem Phys 88: 7242
61. Schweizer KS, Curro JG (1989) J Chem Phys 91: 5059
62. Curro JG, Schweizer KS (1990) Macromolecules 23: 1402
63. Curro JG, Schweizer KS (1991) Macromolecules 24: 6736
64. Kirkwood JG, Buff FP (1951) J Chem Phys 19: 774
65. Chen XS, Forstmann F (1992) J Chem Phys 97: 3696; Malescio G (1992) J Chem Phys 96: 648, and references cited therein; Arrieta E, Jedrzejek C, Marsh KN (1991) ibid 95: 6806 and 6838
66. Sanchez IC (1991) Macromolecules 24: 908
67. Schweizer KS (1993) Macromolecules 26: 6033 and 6050
68. Schweizer KS, Yethiraj A (1993) J Chem Phys 98: 9053

69. Yethiraj A, Schweizer KS (1992) J Chem Phys 97: 5927
70. (a) Yethiraj A, Schweizer KS (1993) J Chem Phys 98: 9080; (b) Singh C, Schweizer KS, Yethiraj A (1994) J Chem Phys, submitted
71. Honeycutt JD (1992) ACS Polymer Preprints 33(1): 529; (1992) Proc. of CAMSE'92, Yokohama, Japan, in press; private communication
72. Singh C, Schweizer KS (1994) J Chem Phys, submitted
73. Deutsch H-P, Binder K (1992) Europhysics Lett 17: 697; (1993) Macromolecules 25: 6214; (1993) J Phys II France 3: 1049, see also, Sariban A, Binder K (1988) Macromolecules 21: 711
74. Gehlsen MP, Rosedale JH, Bates FS, Wignall GD, Hansen L, Almdal K (1992) Phys Rev Lett 68: 2452
75. Chandler D (1993) Phys Rev E 48: 2898
76. Melenkevitz J, Curro JG (1994) in preparation
77. Andersen HC, Chandler D (1972) J Chem Phys 57: 1918, 1930
78. Lupkowski M, Monson PA (1987) J Chem Phys 87: 3618
79. Ladanyi BM, Chandler D (1975) J Chem Phys 62: 4308
80. Dudowicz J, Freed KF (1990) Macromolecules 23: 1519; Tang H, Freed KF (1991) Macromolecules 24: 958
81. Rowlinson JS, Swinton FL (1982) Liquids and Liquid Mixtures, Butterworth Scientific, London
82. Hildebrand J, Scott R (1949) The Solubility of Nonelectrolytes, 3rd Edition, Reinhold, New York
83. Bates FS, Schulz MF, Rosedale JH (1992) Macromolecules 25: 5547
84. Liu AJ, Fredrickson GH (1992) Macromolecules 25: 5551
85. Yethiraj A, Schweizer KS (1993) Bull Am Phys Soc 38(1), 485; David EF, Schweizer KS (1994) in preparation
86. David EF, Schweizer KS (1994) J Chem Phys 100: May 15
87. Leibler L (1980) Macromolecules 13: 1602
88. Fried H, Binder K (1991) J Chem Phys 94: 8349
89. Fredrickson GH, Helfand E (1987) J Chem Phys 87: 697; Brazovski SA (1975) Sov Phys JETP 41: 85
90. Tang H, Freed KF (1992) J Chem Phys 96: 862
91. (a) Yethiraj A, Kumar S, Hariharan A, Schweizer KS (1994) J Chem Phys 100: 4691; (b) Yethiraj A, Hall CK, Dickman R (1992) J Colloid and Interface Sci 151: 102
92. Schweizer KS, Honnell KG, Curro JG (1992) J Chem Phys 96: 3211
93. Chandler D, Singh Y, Richardson DM (1984) J Chem Phys 81: 1975; Nichols AL, Chandler D, Singh Y, Richardson DM (1984) ibid 81, 5109; Laria D, Wu D, Chandler D (1991) ibid, 95: 4444
94. Chandler D (1987) Chem Phys Lett 139: 108
95. Singh Y (1987) J Phys A-Math Gen 20: 3949
96. Melenkevitz J, Schweizer KS, Curro JG (1993) Macromolecules 26: 6190
97. Grayce CJ, Schweizer KS (1994) J Chem Phys 100: May 1
98. Melenkevitz J, Curro JG, Schweizer KS (1993) J Chem Phys 99: 5571
99. Grayce CJ, Yethiraj A, Schweizer KS (1994) J Chem Phys 100: May 1
100. Schweizer KS (1986) J Chem Phys 85: 1156, 1176; Synthetic Metals 28: C565 (1989)
101. Grayce CJ, Schweizer KS (1993) Bull Am Phys Soc 38(1), 485; Macromolecules to be submitted.
102. Melenkevitz J, Muthukumar M (1991) Macromolecules 24: 4199
103. Schweizer KS (1989) J Chem Phys 91: 5802 and 5822; J Non-Cryst Sol 131–133, 643 (1991); Physica Scripta (1993) T49: 99
104. Chiew YC (1990) Mol Phys 70: 129 and 73: 359 (1991); J Chem Phys 93: 5067 (1990).
105. Lipson JEG (1991) Macromolecules 24: 1334; Lipson JEG, Andrews AA (1992) J Chem Phys 96: 1426
106. Gan HH, Eu BC (1993) J Chem Phys 99: 4084, 4103
107. Schweizer KS, Curro JG, Ann Rev Phys Chem, in preparation
108. Curro JG (1994) Macromolecules, in press
109. Donley JP, Curro JG, McCoy JD (1994) J Chem Phys, in press; Sen S, Cohen JM, McCoy JD, Curro JG (1994) J Chem Phys, submitted

Received July 1993